Biochimica et Biophysica Acta 1798 (2010) 750–765

Contents lists available at ScienceDirect

Biochimica et Biophysica Acta

journal homepage: www.elsevier.com/locate/bbamem

Review

Nanoscale analysis of supported lipid bilayers using atomic force microscopy

Karim El Kirat [a,*], Sandrine Morandat [b], Yves F. Dufrêne [c]

[a] Laboratoire de Biomécanique et Bioingénierie, UMR-CNRS 6600, Université de Technologie de Compiègne, BP 20529, F-60205 Compiègne Cedex, France
[b] Laboratoire de Génie Enzymatique et Cellulaire, UMR-CNRS 6022, Université de Technologie de Compiègne, BP 20529, F-60205 Compiègne Cedex, France
[c] Unité de chimie des interfaces, Université catholique de Louvain, Croix du Sud 2/18, B-1348 Louvain-la-Neuve, Belgium

ARTICLE INFO

Article history:
Received 16 June 2009
Received in revised form 17 July 2009
Accepted 23 July 2009
Available online 6 August 2009

Keywords:
Atomic force microscopy
Biomembranes
Nanoscale organization
Real-time imaging
Supported lipid bilayers

ABSTRACT

During the past 15 years, atomic force microscopy (AFM) has opened new opportunities for imaging supported lipid bilayers (SLBs) on the nanoscale. AFM offers a means to visualize the nanoscale structure of SLBs in physiological conditions. A unique feature of AFM is its ability to monitor dynamic events, like bilayer alteration, remodelling or digestion, upon incubation with various external agents such as drugs, detergents, proteins, peptides, nanoparticles, and solvents. Here, we survey recent progress made in the area.

Contents

1. Introduction

Supported lipid bilayers (SLBs), also known as supported planar bilayers or in-plane bilayers, are robust biomimetic model systems that are largely used to study the biophysical and biochemical properties of biological membranes [1,2]. SLBs are also important tools for nanobiotechnology applications, e.g. for the design of patterned biosurfaces with given functionalities [1–6].

The most prevalent methods available to form SLBs are the Langmuir–Blodgett (LB) and Langmuir–Schaefer (LS) techniques, and the fusion of lipid vesicles (Fig. 1). In the LB method (Fig. 1A) [7], a monolayer of lipids is compressed on an aqueous subphase by the moveable barriers of a Langmuir trough made of teflon. Lipid molecules are usually spread at the air–water interface in hexane/ethanol or chloroform/methanol mixtures. After the complete evaporation of the solvent, which generally takes 15 min, the lipid monolayer is compressed (Fig. 1A). A tensiometer records the surface pressure at the air/water interface. Compression/decompression isotherms are obtained by plotting the surface pressure as a function of the interfacial area. Such isotherms provide useful information on the physical state, the packing and the organization of the lipid molecules. The LB technique allows one to transfer the monolayer of amphiphilic molecules onto a solid support, usually mica, at constant surface pressure and constant speed (Fig. 1A). Careful control of surface pressure and lifting speed is essential to avoid artefacts such as

* Corresponding author. Tel.: +33 3 44 23 73 56; fax: +33 3 44 23 79 42.
E-mail address: kelkirat@utc.fr (K. El Kirat).

0005-2736/$ – see front matter
doi:10.1016/j.bbamem.2009.07.026

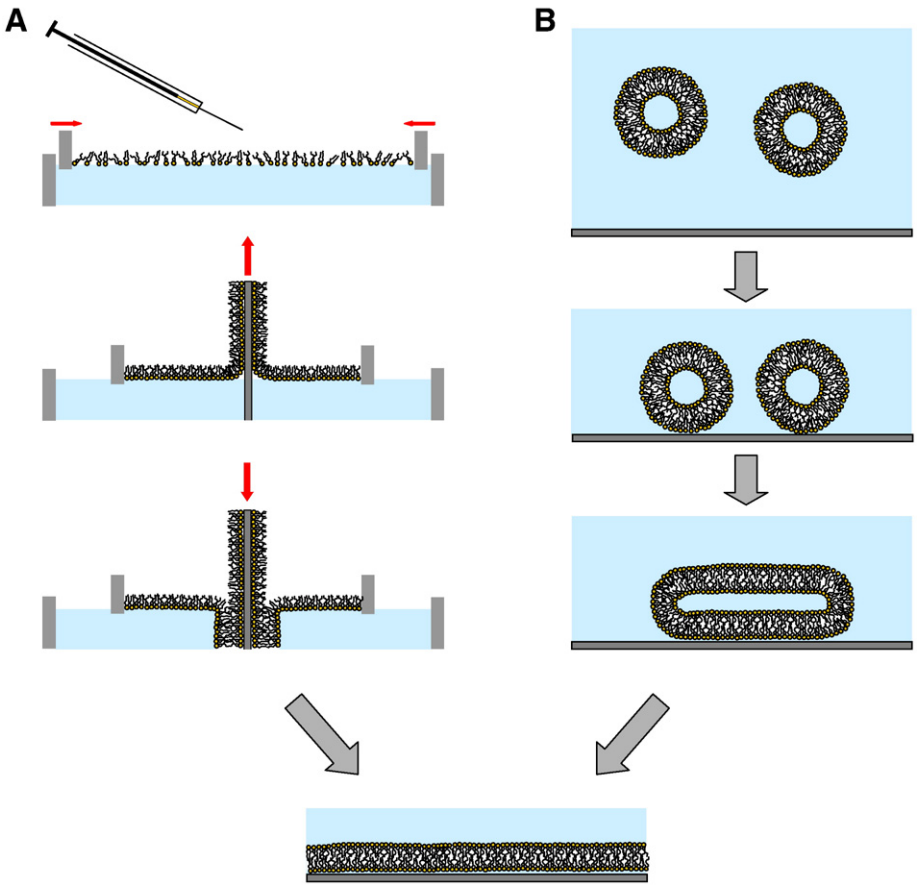

Fig. 1. Preparation of bilayers for AFM studies. Two methods commonly used for preparing SLBs: (A) Langmuir–Blodgett technique and (B) fusion of lipid vesicles.

defect formation or feature alignment of the deposited structures [8]. If the solid support is hydrophilic, such as mica, the lipid polar heads interact with the support, thus exposing the hydrophobic tails to the environment. Supported monolayers are stable in air, not in water, and should therefore be examined in air. To better mimic cellular membranes, a supported bilayer can be formed by transferring a second lipid layer onto the first mica-supported lipid monolayer (Fig. 1A). Supported bilayers should always be kept and analyzed in aqueous solution since they are not stable in air. The second lipid monolayer transferred can be of different composition, thus yielding asymmetric SLBs [9,10].

The fusion of lipid vesicles on solid supports is the most simple and popular method for preparing SLBs (Fig. 1B) [11–14]. To prepare vesicles, the lipids are first solubilized in organic solvent. After solvent evaporation under nitrogen and subsequent desiccation under vacuum, the dried lipid film is resuspended in an aqueous buffer solution yielding a multilamellar vesicle (MLVs) suspension. Small unilamellar vesicles (SUVs) can then be obtained using various approaches, sonication of the MLVs being the most popular one. The suspension is sonicated to clarity using a titanium probe sonicator while keeping the suspension in an ice bath, after which the suspension is filtered on nylon filters to eliminate titanium particles. The fusion step is achieved by depositing the SUV suspension onto freshly cleaved mica for 45–60 min at 45–60 °C, which is generally above the melting temperature of the lipids. The SLBs are finally gently cooled to room temperature and rinsed abundantly with the appropriate image buffer to remove unfused vesicles. The mechanism of bilayer formation from SUVs is not fully understood yet. The following steps are generally admitted to describe the transition from SUVs to SLBs: adsorption of the vesicles on the surface, deformation, flattening and finally rupture to form a continuous SLB (Fig. 1B) [13,14]. In addition, the speed of the bilayer formation and the overall morphology strongly depend on lipid composition and concentration, temperature, electrostatic effects, solid support and presence of divalent cations (particularly Ca^{2+}) [14–16]. Unlike LB deposition, the fusion method cannot be used to prepare asymmetric bilayers composed of two layers of different nature. However, the fusion approach is remarkably simple, and the lateral mobility of the lipids is only slightly slower than in giant unilamellar vesicles [17], meaning these membranes are more biologically relevant.

Note that besides these two frequently used methods, there are alternative ways to prepare SLBs, such as for instance the hydration of spin-coated films [18–20]. Lipid molecules are dissolved in an organic solvent that is able to wet the solid support. The lipid solution is deposited on the rotating support to evaporate the solvent which produces a uniform dry film. Then, the lipid film is hydrated with buffer. This method is suitable to prepare lipid bilayers with a full coverage of the support. However, superimposed bilayers are often formed and the number of bilayers ranges between 2 and 30. The number of stacked bilayers depends on the concentration of the lipid solution [19].

To preserve the structural and functional properties of SLBs, they must be protected from dewetting. Indeed, the structure of SLBs is dramatically altered when they are exposed to air. Protective agents can be used to prevent dehydration damages and to increase the stability of SLBs [21,22]. Sucrose and trehalose seem to provide the best protective effects on SLBs against the dehydration stress. Furthermore, these two disaccharides also preserve the overall integrity of the SLBs by preventing fusion and enlargement of microdomains [21,22].

A wide variety of techniques are available to probe the structure, composition and properties of lipid films in non-supported monolayers

and in vesicles, including fluorescence [23] and Brewster angle microscopy [24], X-ray reflection [25] and diffraction [26] methods, neutron reflectivity [27], and nuclear magnetic resonance [28,29]. Transferring lipid films onto solid substrata offers the possibility to apply a range of surface analytical techniques that could not be used to study real biological membranes, such as ellipsometry [30], X-ray photoelectron spectrometry [31], fluorescence recovery after photobleaching [32] and time-of-flight secondary ion mass spectrometry [33]. However, until recently little was known about the nanoscale structure of SLBs, and their real-time remodelling, due to a lack of in situ, high-resolution surface imaging techniques.

This challenge can now be addressed owing to the advent of atomic force microscopy (AFM) [34]. Compared to other microscopies, AFM offers the key advantage that the structure of biological samples like cells and lipid membranes can be explored in real-time with (sub) nanometer resolution [35,36].The basic idea behind AFM is to scan a sharp tip over the surface of a sample, while sensing the interaction force between the tip and the sample. This allows three-dimensional images to be generated directly in aqueous solution. The sample is mounted on a piezoelectric scanner which ensures three-dimensional positioning with high accuracy. While the tip (or sample) is being scanned in the (x, y) directions, the force interacting between tip and specimen is monitored with piconewton sensitivity. This force is measured by the deflection of a soft cantilever which is detected by a laser beam focused on the free end of the cantilever and reflected into a photodiode.

Different AFM imaging modes are available, which differ mainly in the way the tip is moving over the sample. In the so-called contact mode, the AFM tip is raster scanned over the sample while the cantilever deflection, thus the force applied to the tip, is kept constant using feedback control. In dynamic or intermittent mode, such as tapping mode, an oscillating tip is scanned over the surface and the amplitude and phase of the cantilever are monitored near its resonance frequency. Because lateral forces during imaging are greatly reduced with dynamic modes, they are advantageous for imaging soft biological samples.

Besides structural imaging, AFM can be used in the force spectroscopy mode to probe molecular forces, chemical properties and receptor sites. Although of great potential, the use of force spectroscopy in SLB research remains rather limited [10,37–43] and will therefore not be covered here.

2. AFM reveals the nanoscale organization of lipid bilayers

Within 15 years, AFM has become a well-established technique for imaging the lateral organization of phase-separated SLBs. In a pioneering study, hydrated bilayers made of a mixed (19:1) upper layer of 1,2-dimyristoyl-sn-glycero-3-phosphoethanolamine (DMPE) and biotinylated 1,2-palmitoyl-sn-glycero-3-phosphoethanolamine (DPPE) on DPPE-coated mica were imaged, revealing the coexistence of fluid and crystalline domains [44]. Since then, many phase-separated SLBs made of binary mixtures have been investigated [10,45–48]. As a typical example, Fig. 2 shows the topographic image obtained for mixed 1,2-dioleoyl-sn-glycero-3-phosphocholine/1,2-plamitoyl-sn-glycero-3-phosphocholine (DOPC/DPPC) (1:1, mol/mol) bilayers in buffer. The image reveals the coexistence of two phases. Considering the phase diagrams of these two lipids, the brighter levels can be ascribed to DPPC in the gel phase (also called solid S phase) and the darker surrounding matrix to DOPC in the fluid phase (also called liquid disordered Ld phase). The step height measured between the two phases is 1.1 ± 0.1 nm and results from a difference in the thickness and mechanical properties of the DOPC and DPPC films.

Using a temperature controlled stage, the time-dependent remodelling of SLBs can be directly visualized by AFM. For instance, this approach was used to study the structure and kinetics of ripple

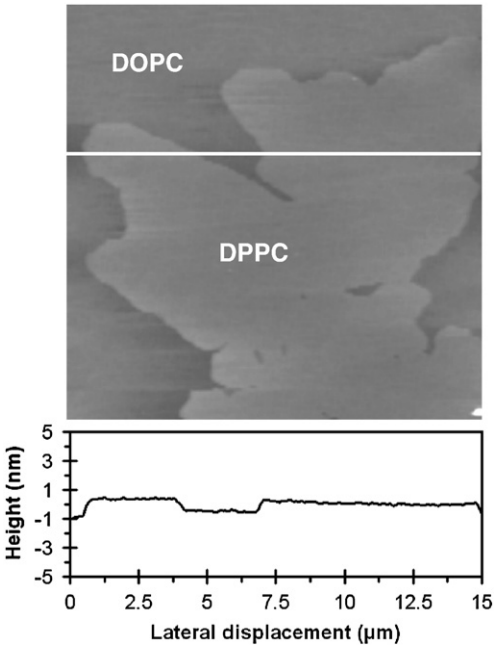

Fig. 2. Domain formation in fluid/gel SLBs. AFM topographic images (15 μm × 15 μm, z-range of 10 nm) of a DOPC/DPPC (1:1 molar ratio) bilayer recorded in Tris 10 mM, NaCl 150 mM buffer (pH 7.4). A cross section taken along the white line is shown beneath the image.

phases in DPPC bilayers [49,50]. The bilayer systems were mica-supported double bilayers in which the top bilayer formed ripple phases. Depending on both their amplitude and period, three different types of ripples were distinguished. Importantly, the conversion of the different types of ripples was thermally tuned. The 2Λ-ripple had an amplitude of $A \geq 110$ Å and a periodicity of ~550 Å. The two other ripples Λ and $\Lambda/2$ presented an amplitude of $A \geq 50$ Å and $A \geq 12$ Å, respectively, and a period of about 280 and 150 Å. It is worth noting that ripple phases were also observed on single SLBs of 1,2-myristoyl-sn-glycero-3-phosphocholine/1,2-stearoyl-sn-glycero-3-phosphocholine (DMPC/DSPC) SLBs [51].

AFM also permitted to address the important issues of nucleation and growth of laterally segregated domains in SLBs [45,47,52–55]. While most studies on model SLBs have demonstrated the formation of domains that display complete transmembrane symmetry, only few reports have dealt with more biologically relevant asymmetric membrane structures. Indeed, transmembrane asymmetry is a fundamental property of cell membranes. The compositional asymmetry and the nucleation of gel domains in DOPC/DPPC SLBs were observed by real-time AFM by decreasing the temperature from 60 to 23 °C [45]. The growth rates of the DPPC gel domains were dependent on the coupling between the two leaflets of the bilayer. More recently, the same compositional asymmetry was evidenced on DOPC/DPPC SLBs for short equilibration times [56]. In 2006, the Longo's team extensively examined the influence of the protocol of fusion on the asymmetry of SLBs [47]. Vesicles were composed of 1,2-lauroyl-sn-glycero-3-phosphocholine (DLPC)/DSPC mixtures and SUVs were obtained either by extrusion or sonication. The extruded SUVs were heated at 65 °C and deposited on mica for fusion at 20 °C. AFM images showed the formation of fully symmetric bilayers of DLPC/DSPC fluid/gel SLBs. Concerning the SUVs obtained by sonication, the resulting SLBs were always asymmetric. When sonicated SUVs were heated at 20 °C prior to fusion, the SLBs were completely asymmetric, while sonicated SUVs heated at 65 °C formed partially symmetric SLBs. For the two methods giving totally symmetric or totally asymmetric bilayers, the DSPC domains protruded from the DLPC phase by 1.8 nm and 1.1 nm respectively and they were always stable over a period of 4 h.

Recently, in a study by Bernchou et al. [55], the formation of DPPC-enriched domains was shown to proceed by a nucleation mechanism proportional to the cooling rate of the sample. During the cooling step from 31 to 16 °C, the shape of the DPPC domains evolved from a round to a "fractal" morphology. The authors suggested that the growth of the domains was controlled by the diffusion of DPPC from the liquid phase toward the gel domain interface. According to Blanchette et al. [52], the solid support under the membrane directly influences the number of nucleation sites. The rate of sample cooling after the fusion of SLBs modifies the size and shape of galactosylceramide (GalCer) domains in a DLPC membrane.

In the past decade, there has been increasing evidence suggesting that lipids of the cell membrane might be organized into small lipid domains which are in a physical state similar to a liquid-ordered (Lo) phase, surrounded by lipids in a Ld phase [57]. The Lo phase is characterized by a high packing of the lipid acyl chains but also a high lipid mobility that is similar to that of Ld bilayers [58,59]. In this context, AFM has been widely used to study complex lipid mixtures displaying both Lo and Ld phases [52,60–66]. Ternary lipid mixtures containing saturated phosphatidylcholine (PC) or sphingomyelin (SM), an unsaturated PC, and Cholesterol (Chol) have been shown to exhibit two coexisting fluid phases: a Lo phase that is enriched in Chol and SM or saturated PC and a Ld phase that is predominantly composed of unsaturated PC [48]. In 2001, Rinia et al. [60] described the preparation of SLBs composed of DOPC/SM 1:1 (mol/mol) and different percentages of Chol. They observed that the morphology and the size of the domains depend directly on the Chol content. Indeed, for the binary DOPC/SM mixture, they obtained gel domains of SM surrounded by fluid areas of DOPC and an intermediate level corresponding to the asymmetry of composition in the upper and lower leaflets of the SLB. The addition of Chol to the bilayer between 5 and 15% inhibited the formation of asymmetric domains without changing their global shape suggesting that Chol may participate in the coupling of the two leaflets of the membrane [60,66]. Above 15% of Chol in the SLBs, the size of the domains increased with the Chol content and the height difference between the fluid phase and the domains decreased [60].

Ceramides are sphingolipids playing important structural and biological roles in natural membranes [67–69]. GalCer, which belongs to the glycosphingolipid family, was postulated to be associated with the Lo domains in the cell membranes [70]. Blanchette et al. [52] investigated the impact of Chol on the formation of GalCer domains. By using DLPC/GalCer/Chol mixtures, they observed that this ternary mixture only displays Ld/S coexistence and no Lo phase even at high Chol content. By measuring the area/perimeter ratios of the segregated domains, the authors deduced that Chol was able to decrease the line tension between the two phases. Chol reduced the time required to reach the equilibrium, i.e. the stabilization of the segregated domains in small microstructures. The same team described the influence of the unsaturation level of PC acyl chains on the obtention of a Lo phase in ternary mixtures containing GalCer and Chol [62]. They obtained a coexistence of Ld/Lo phases with POPC and DOPC at 10 mol% Chol. These results highlight the importance of fatty acyl chain unsaturation, sterol content and lipid hydrophobic mismatch in the organization of multi-component lipid systems. Chiantia et al. [63,64] combined AFM, confocal fluorescence and fluorescence correlation spectroscopy (FCS) to probe bilayers containing SM/DOPC/Chol/ceramide. According to their findings, such membrane composition exhibits a coexistence of three different phases: Ld enriched in DOPC, Lo of SM and Chol, and ceramide-rich gel domains.

Other complex mixtures have also been investigated. For instance, the Hernandez-Borrell's team recently examined the properties of SLBs formed from three phospholipid components that comprise the mitochondrial inner membrane, i.e. 1-palmitoyl-2-oleoyl-sn-glycero-3-phosphocholine (POPC), 1-palmitoyl-2-oleoyl-sn-glycero-3-phosphoethanolamine (POPE) and cardiolipin (CL) [71]. They observed: (i) that the thickness of the bilayers, calculated from cross-sectional analyses, decreased with increasing temperatures; (ii) the existence of laterally segregated domains that respond to temperature; (iii) a decrease in height and an increase in roughness of SPBs after cytochrome *c* injection at room temperature.

Several researcher teams have also investigated the influence of ions or solvents on the organization of SLBs. For instance, Ca^{2+} was shown to have a dramatic effect on the structure of phase-separated bilayers containing mixtures of phospholipids in gel (DPPC) and fluid (1,2-dioleoyl-sn-glycero-3-phosphoserine, DOPS, or DOPC) states [72]. In the absence of Ca^{2+}, large, well-defined DPPC domains were found in both the DPPC/DOPC and DPPC/DOPS mixtures, while in its presence, small isolated DPPC domains were found in the DPPC/DOPS mixture. Ca^{2+} had no effect on the organization of DPPC in DPPC/DOPC mixtures, and its effect was abolished by adding DOPC to DPPC/DOPS mixtures. In another work, Mou et al. [73] showed that low percentages of ethanol induce interdigitation in DPPC supported bilayers. In 2001, McClain and Breen [74] described the interdigitation of DPPC bilayers induced by another alcohol: 2-propanol. They also observed that this interdigitation was reversible but the transition from one state to the other was very slow (hours to days) for membranes in the gel phase. The commonly used buffer compound Tris (tris(hydroxymethy1)aminomethane) was found to induce a ripple phase in supported 1,2-dipentadecanoyl-sn-glycero-3-phosphatidylcholine bilayers [75]. The ripple structure showed various types of domains that could extend to several micrometers in length with changes in direction with angles of 120° and 60° that are characteristic of PC ripple phases. An interesting direction for future SLB research would be to study the influence of support chemistry and roughness on bilayer formation, a topic that has recently received increasing interest (for review see [54]).

3. AFM monitors bilayer–detergent interactions

Detergents are important tools in biology for the fractionation and reconstitution of membrane components, with the aim to perform biophysical and structural studies of biological membranes and proteins. It is now well-established that the plasma membrane of eukaryotic cells is not homogeneously organized as proposed by the fluid mosaic model [76]. In fact, these membranes present microdomains also called "rafts" that are especially enriched in sphingolipids and cholesterol (Chol) [77,78]. Membrane microdomains play a pivotal role in many important cellular processes such as signal transduction and membrane trafficking [79–83]. Generally, rafts can be purified as detergent resistant membranes (DRMs) by cold extraction (4 °C) with the non-ionic detergent Triton X-100 (TX-100) of eukaryotic cell plasma membranes [78,80,84–86]. Accordingly, the solubilization of biological membranes by detergents constitutes an important issue.

Owing to their conical molecular structure, detergents molecules have a positive, spontaneous curvature and, therefore, they tend to form small spherical structures with a highly curved surface (micelles). The solubilization of vesicles is an all-or-none mechanism which is generally described as a three-stage process [87–89]. During the first stage, when the detergent is added at low concentration to biomembranes, the detergent molecules are partitioned between the aqueous medium and the phospholipid bilayers. The progressive insertion of individual molecules of detergent provokes the swelling of the vesicles. At stage II, by increasing detergent concentration, some mixed micelles of lipid–detergent dissociate from the detergent-saturated membranes thus resulting in a decrease of the turbidity. The stage III is reached at higher detergent concentrations, the vesicles are then completely solubilized and all the phospholipid molecules reside in curved, mixed lipid–detergent micelles.

The solubilization of SLBs by detergents was visualized by AFM for the first time in 2001 [60]. A DOPC/SM bilayer with 25% Chol treated with TX-100 at 4 °C clearly showed that the fluid phase disappeared while the ordered SM/Chol domains remained unchanged. More recently, the TX-100 solubilization of DOPC/DPPC 1:1 (mol/mol) bilayers was investigated by time-lapse AFM [90]. When TX-100 was added above its critical micelle concentration (CMC), it was able to dramatically impair the DOPC/DPPC bilayers by instantly removing the DOPC fluid phase. The remaining DPPC gel patches appeared then more or less swollen depending on the initial TX-100 concentration. The swelling of the gel domains was directly correlated with detergent intercalation between DPPC molecules. Finally, the remaining swollen DPPC patches were crumbled by the sporadic desorption of bilayer parts, ultimately leaving a global silhouette on the mica which was reminiscent of the initial gel phase. The solubilization of these fluid/gel SLBs was also studied with the n-octyl β-D-glucopyranoside (OG) detergent [91]. OG and TX-100 belong to the same class of non-ionic detergent and they seem to solubilize membranes in the same manner at the macroscopic scale [87–89]. However, AFM experiments permitted to point out remarkably strong differences in their respective mechanisms of membrane solubilization [91]. Just after OG addition, the bilayer was completely desorbed from the mica and no material remained on the surface. Surprisingly, the lipids solubilized by OG were then able to sediment and fuse on the solid support thus regenerating a new SLB. Another team [92,93] described the interaction of different sugar-based detergents with DOPC/DPPC SLBs. They observed that at room temperature and at concentrations above their CMC, SLBs were more resistant to dodecyl β-D maltoside (DDM) and dodecyl β-D thiomaltoside (DOTM) as compared to OG. The authors also evidenced that a concentration of 5 mM in calcium ions has a protective effect on the solubilization process by increasing the lateral packing of lipids [93].

The solubilization of more complex lipid mixtures by TX-100 was also examined with the help of time-lapse AFM to understand the influence of Chol in the resistance of lipid rafts to detergent extraction [65]. To this end, three types of bilayers were prepared: DOPC/SM 1:1 (mol/mol), DOPC/SM/Chol 2:1:1 (mol/mol/mol) or 4:3:1 (mol/mol/mol). At a concentration above the CMC of TX-100, whatever the lipid composition, the first step of the solubilization always consisted in the complete removal of the DOPC fluid phase. The solubilization of fluid/gel DOPC/SM bilayers was similar to the one observed with DOPC/DPPC by the sporadic removal of bilayer patches from the remaining SM gel domains, ultimately leaving crumbled domains with their silhouette reminiscent of the initial SM gel phase. The major difference between the solubilization of DOPC/DPPC and DOPC/SM bilayers was the absence of swelling of the gel remaining domains. When the raft mimicking membranes DOPC/SM/Chol 2:1:1 (mol/mol/mol) were incubated with TX-100, no holes could be observed in the Lo SM/Chol patches. The Lo patches were eroded progressively from their edges where the lipid packing was disturbed. No hole was seen with this raft composition of lipids. By contrast, with an intermediate mixture of DOPC/SM/Chol 4:3:1 (mol/mol/mol), the remaining patches enriched in SM/Chol were modified by both the hole formation and the erosion. This intermediate mixture confirms the requirement for a minimum amount of Chol mixed with SM to provide a good resistance to TX-100 solubilization.

By mixing detergents and lipids before the preparation of SLBs, it is possible to obtain highly organized patterns embedded in the bilayer. These membrane systems are suitable for high-resolution imaging of detergent enriched domains [94]. Liposomes of pre-mixed DPPC-detergent were fused on a mica support. It was shown that both detergents TX-100 and Tween-20 produced ordered patterns (Fig. 3) very similar to the striated domains described previously with helical peptides [95,96]. Indeed, line-type depressions and elevated lines were observed with different morphologies depending on the nature of the detergent. The line-type depressions were attributed to dimers of detergent inserted in DPPC in a head to tail fashion.

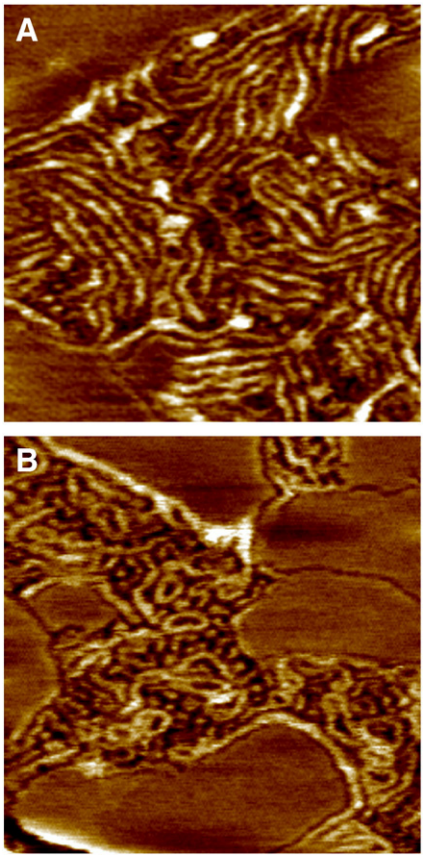

Fig. 3. Formation of highly ordered domains of detergents in DPPC bilayers. AFM images of DPPC bilayers presenting striated domains induced by 10 mol% of TX-100 (A) and 2.5 mol% of Tween 20 (B) (750 nm × 750 nm, *z*-scale = 1.5 nm). Adapted with permission from [94]. Copyright 2008 Inderscience Enterprises Ltd.

4. AFM visualizes the interaction of lipid bilayers with peptides

Membrane–peptide interactions play essential roles in a number of biological events, including membrane fusion and membrane lysis [97,98]. In this context, AFM is increasingly used to observe, in aqueous solution, the effect of peptides on the nanoscale structure of SLBs. Examples of peptides that have been investigated so far include model peptides, antimicrobial peptides, virus-derived peptides, cell-penetrating peptides and amyloid peptides.

In pioneering work, Rinia and co-workers provided evidence for the formation of striated domains of model peptides within DPPC bilayers [95,96]. These peptides consisted of the same alanine–leucine stretch and either tryptophans, tyrosines, phenylalanines, lysines or histidines as flanking residues. According to this study, the occurrence of striated domains strongly depended on the nature of the flanking residues. In 2005, Pedersen et al. [99] described the nanoscale structure of DPPC membranes incorporated with a synthetic decapeptide N-terminally linked to a C_{14} acyl chain (C_{14}-peptide). They found that the C_{14}-peptide inserts preferentially into pre-existing defect regions and displays a membrane thinning effect on the surrounding lipids.

Regarding antimicrobial peptides, Mou et al. showed that the interaction between gramicidin A (gA) and DPPC bilayers leads to the formation of highly ordered domains [100]. Peptides were self-assembled into line-type aggregates and these aggregates clustered together to form the ordered domains. This organization was attributed to the ability of gA to span bilayers as a β-helical dimer. The amphipathic membrane-active peptide melittin extracted from bee venom was shown to cause dramatic disruption of lipid bilayers [101]. An analog of magainin 2, which is an antimicrobial peptide isolated from the skin of the African clawed frog *Xenopus laevis*, promoted the thinning of 1.1 nm

in distinct areas of a DMPC membrane [102]. AFM imaging also provided a glimpse into the membrane selectivity of antimicrobial peptides. For indolicidin, an antimicrobial peptide extracted from bovine neutrophils, the mechanism of action is modulated by the concentration, the charge and phase of the lipids, and the cholesterol content. At low concentrations of this peptide, AFM imaging revealed the formation of carpet-like layers on fluid cationic lipid membranes. By contrast, a thinning of the lipid gel domains was observed at high peptide concentrations [103].

How about virus-derived peptides? In early work, tapping mode AFM imaging revealed the real-time self-assembly within SLBs of two peptides derived from hemagglutinin, a protein of the common flu virus Influenza [104]. More recently, AFM provided novel insight into the membrane interactions of tilted peptides. Tilted peptides represent a special class of fusogenic peptides in many membrane-interacting proteins such as viral fusion proteins, neurotoxic proteins and proteins involved in lipoprotein metabolism [105–107]. These short peptides (10 to 20 residues) have a hydrophobicity gradient that runs along the axis of their helical structure. Hence, their hydrophobicity increases from one end of the helix to the other, a property that causes them to insert at an angle of 30–60° in lipid membranes. In the first AFM study, nanoscale surface imaging was used to demonstrate that the tilted peptide derived from the Simian Immunodeficiency Virus (SIV) induces stable nanoholes in lipid bilayer domains [108]. These observations are very similar to the results of Lev and Shai [109] with a fusion peptide derived from the Human Immunodeficiency Virus (HIV). Incubation of preformed DOPC/DPPC bilayers with SIV led to the rapid appearance of nanometer scale holes within DPPC gel domains, while keeping the domain shape unaltered. This behaviour was attributed to a local weakening and destabilization of the gel domains due to the oblique insertion of peptides and it was directly correlated with the fusogenicity of the SIV tilted peptide.

According to the generally admitted stalk mechanism described for membrane fusion, negatively curved lipids may play a central role during the early steps of the fusion process [110,111]. In this context, AFM enabled to address the crucial question of whether negatively curved lipids influence the interaction of the SIV fusion peptide with model membranes (Fig. 4) [112]. To this end, DOPC/DPPC bilayers containing 0.5 mol% 1,2-dioleoyl-sn-glycero-3-phosphoric acid (DOPA) were incubated with the SIV peptide and imaged using time-lapse AFM. After a short incubation time, a 1.9 nm reduction in the thickness of the DPPC domains was observed, reflecting either interdigitation or fluidization of lipids. After longer incubation times, these depressed DPPC domains evolved into elevated domains, composed of nanorod structures protruding several nanometers above the bilayer surface and attributed to cylindrical reverse micelles. Such DOPC/DPPC/DOPA bilayer modifications were never observed with nontilted peptides.

Cell-penetrating peptides (CPPs) are natural or synthetic water soluble peptides that translocate hydrophilic molecules across cell membranes with high efficiency and low lytic activity. CPPs have been widely used as vectors for cytoplasmic and nuclear delivery of therapeutic compounds. In 2006, Herbig et al. [113] investigated the interaction of two CPPs derived from VE-cadherin with DOPC bilayers containing a gel phase of either DPPC or SM. For the DPPC-containing SLBs, AFM images showed that the gel domains were progressively fluidized by the CPPs, with an intermediate state composed of many branched structures. By contrast, SM gel domains were not transformed due to their higher molecular packing. In fact, the two CPPs studied by Herbig et al. interacted mainly with the fluid/gel interface and, therefore lessened the packing density of the lipids acyl chains. The interaction of another CPP was investigated on PC bilayers [114], AFM images evidenced coexisting long and thin filaments lying flat on the membrane surface and deeply embedded peptides in locally thinned areas of the bilayer.

Several peptides or proteins are able to form amyloid fibrils [115]. The three major examples are amyloid-β (Aβ), human amylin (hA) and the prion protein (PrP) involved in Alzheimer's disease, type 2 diabetes and bovine spongiform encephalopathy, respectively. Therefore, understanding the molecular mechanisms by which amyloid fibrils form and associate with membranes is a highly relevant challenge. Yip and McLaurin observed the formation of fibrils by Aβ peptides (1–42 and 1–40) in association with lipid bilayers [116,117]. They demonstrated the association of Aβ with planar bilayers composed of total brain lipids, yielding to peptide aggregation and eventually to fibre formation. The extent of Aβ-assembly on the membrane surface was modulated by the cholesterol content. More recently, Choucair et al. [56] showed that addition of Aβ(1–42) peptide to preformed DOPC/DPPC SLBs leads to the accumulation of the peptide exclusively on the DPPC gel domains. By contrast, Aβ was randomly distributed in both fluid and gel phases when the peptide was reconstituted into DOPC/DPPC vesicles prior to fusion. The authors suggested that the preferential accumulation of Aβ on gel domains may be relevant to a possible involvement of lipid rafts as platforms modulating Aβ activity *in vivo*. A shorter Aβ peptide was shown to self-assemble into highly ordered parallel arrays of nanofilaments on fluid lipid bilayers [118]. In 2007, the PrP(106–126) peptide derived from the prion protein was investigated in interaction with SLBs by time-lapse AFM [119]. The first step of this interaction consisted in the formation of pores. Then, the peptide underwent a poration-mediated diffusion in the SLBs by the formation and expansion of flat high-rise domains.

Lipopeptides of microbial origin have also been investigated. Surfactins are surface-active lipopeptides produced by *Bacillus subtilis* strains, which are attracting more and more attention due to their high surface activity and remarkable biological properties, including antiviral and antibacterial activities [120]. As the biological activity of surfactin directly relies on its interaction with membranes, understanding the molecular interactions, mixing behaviour and domain formation of this molecule within lipid bilayers is an important challenge. Surfactin was shown to induce nanoripples of 30 nm periodicity in DPPC bilayers at 25°, i.e. well below the pretransition temperature of DPPC [121]. While most undulations formed straight orientation of ripple phases with characteristic angle changes of 120°, as previously observed by AFM, some of them also displayed unusual circular orientations. Ripple structures were formed at 15% surfactin, but were rarely or never observed at 5% and 30% surfactin, emphasizing the important role of surfactin concentration. Theoretical simulations corroborated the AFM data by revealing the formation of stable surfactin/lipid assemblies with positive curvature. To our knowledge these are the first data revealing the formation of a ripple phase induced by a lipopeptide.

In another study, synthetic analogs of surfactins were used to demonstrate the crucial role played by geometry, charge and hydrophobicity in modulating the membrane activity (solubilization, redeposition) of surfactins (Fig. 5) [122]. AFM images of mixed DOPC/DPPC bilayers recorded after injection of cyclic surfactin at 1 mM, i.e. well-above the CMC, revealed a complete solubilization of the bilayers within 30 min. A linear analog having the same charge and acyl chains was able to solubilize DOPC, but not DPPC, and to promote redeposition leading eventually to a new bilayer. Increasing the charge of the polar head or the length of the acyl chains of the analogs lead to the complete solubilization of both DOPC and DPPC, thus to a stronger membrane activity. Lastly, at low surfactin concentrations (40 μM), DPPC domains were always resistant to solubilization.

An important challenge remaining to address in the bilayer-peptide context, is the AFM imaging of voltage-dependent peptides in SLBs under an electric field. Indeed, voltage-dependent peptides can induce the formation of ions channels in membranes by changing their conformation/aggregation when they are submitted to electric fields. In fact, the observation of voltage-induced transitions could be observed in SLBs by AFM with the appropriate imaging cells, as proposed previously [123,124]. The same type of AFM cell could be useful to study ion transports across membranes separating two liquid compartments [125,126].

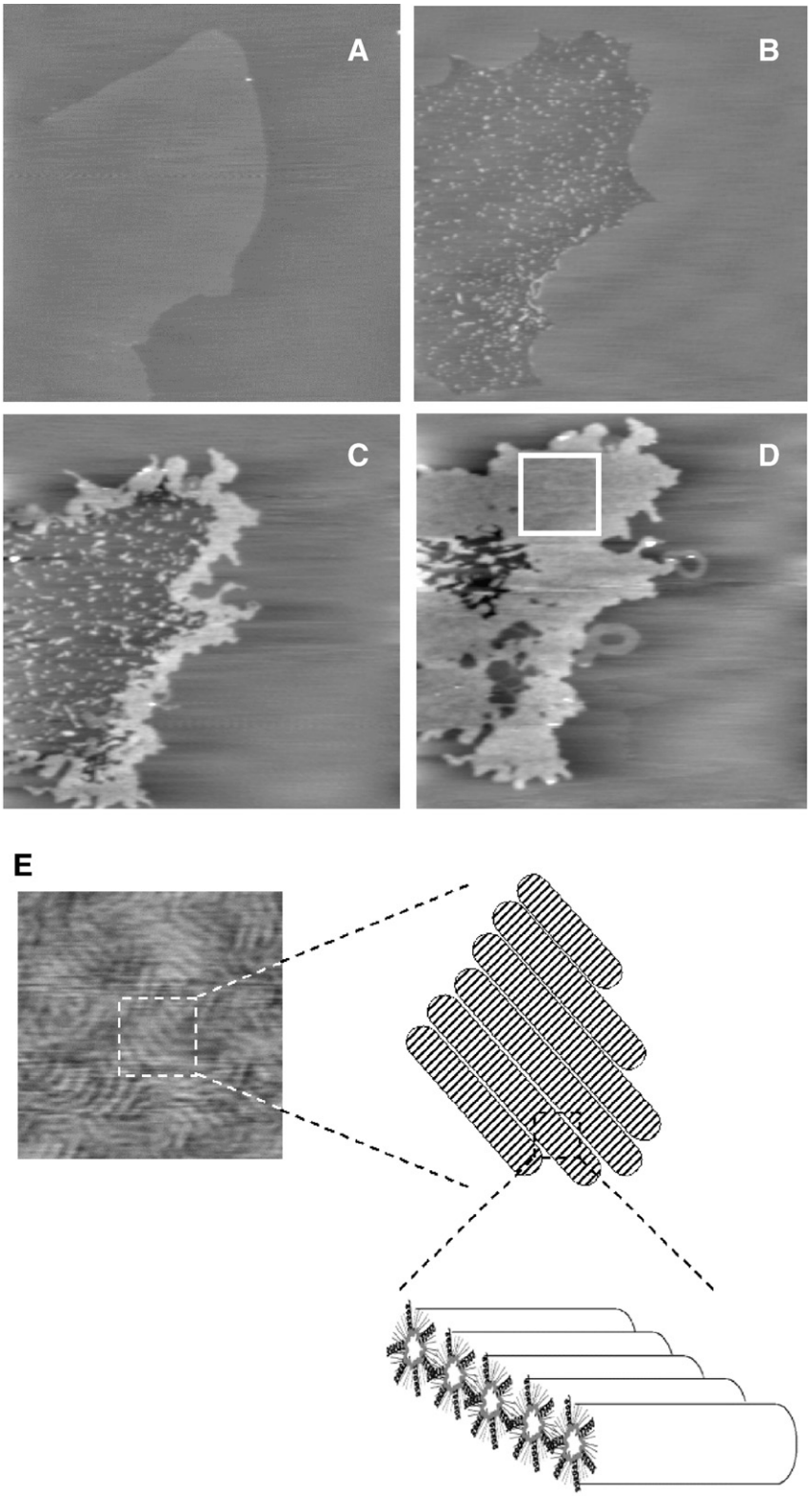

Fig. 4. Influence of the SIV peptide on DOPC/DPPC/DOPA bilayers. AFM topographic images (15 μm × 15 μm, *z*-range of 10 nm) of a DOPC/DPPC/DOPA (495:500:5 molar ratio) bilayer recorded in Tris and EDTA (pH 7.4) (A, 0 min) and in a 10 μM SIV peptide solution (Tris/EDTA) after (B) 15, (C) 40, and (D) 60 min. (E) Higher magnification (3 μm × 3 μm, *z*-range of 2 nm) of the AFM topographic image shown in panel D (white box). Schematic enlargement of the thicker phase showing that it is constructed by self-association of cylindrical reverse micelles having their main axis perpendicular to the main axis of the nanorods that are visible in the AFM image. According to this model, cylindrical reverse micelles present a length of 77 nm, corresponding to the period of the thicker phase composed of nanorods. Adapted with permission from [112]. Copyright 2006 American Chemical Society.

5. AFM observes the interaction of lipid bilayers with proteins

There has also been progress in using AFM to visualize the interaction of proteins with lipid bilayers, a topic which is also highly relevant since the nature as well as the physical state of lipids can modulate the functions of membrane-associated proteins and their ability to assemble into functional oligomers [127]. In one such study, the insertion of the glycosylphosphatidylinositol (GPI)-anchored

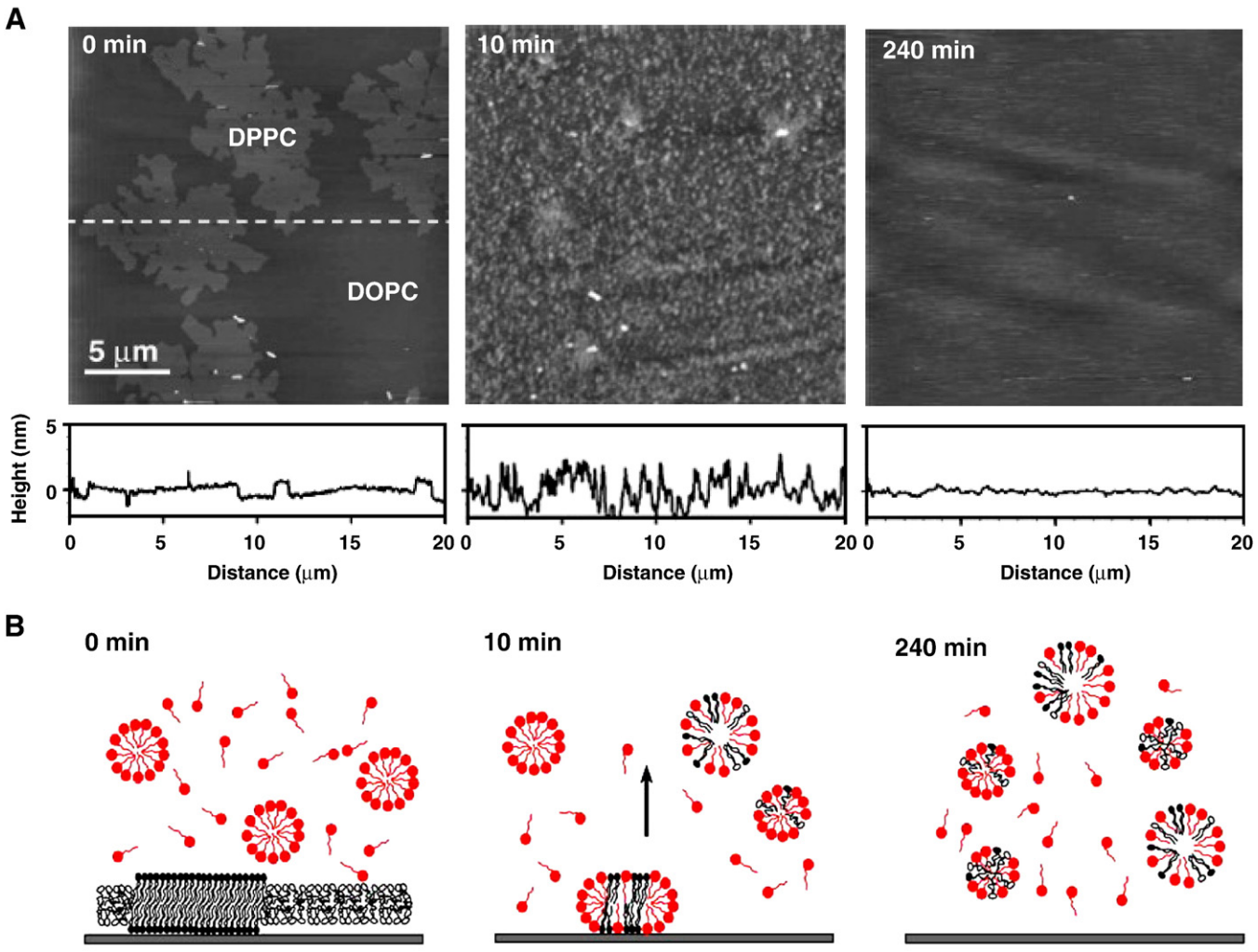

Fig. 5. Nanoscale membrane activity of natural cyclic surfactin. (A) AFM height images (20 μm × 20 μm; z-scale: 20 nm) of a mixed DOPC/DPPC (1:1, mol/mol) bilayer recorded prior (0 min) and after incubation for 10 and 240 min with surfactin at 1 mM. For all images, vertical cross-sections were taken along the position indicated by the dashed line at time 0 min. (B) Molecular model proposed to describe the nanoscale membrane activity of the natural cyclic surfactin at 1 mM. Molecules in red, with a single tail, represent the surfactin molecules, while molecules with double tails and either black or white headgroup represent the DOPC and DPPC lipids. Adapted with permission from [122]. Copyright 2008 Elsevier Science Ltd.

alkaline phosphatase (AP) was studied in real-time in order to understand better how GPI proteins partition into rafts [61,66]. Supported phospholipid bilayers made of a mixture of DOPC/SM containing cholesterol (Chol+) or not (Chol−) were used to mimic the fluid-ordered lipid phase separation in biological membranes. Spontaneous insertion of AP through its GPI anchor was observed inside both Chol+ and Chol− lipid ordered domains, but AP insertion was markedly increased by the presence of cholesterol. More recently [128], the GPI-anchored bovine intestinal alkaline phophatase (BIAP) was shown to be inserted in the gel domains of the three lipid mixtures exhibiting a fluid–gel phase separation: DOPC/DPPC, DOPC/SM and POPC/SM. Moreover, the protein insertion was associated with a remodelling of the gel domains corresponding to a net transfer of phospholipids from one phase to the other. The direction of the transfer was clearly dependent on the constituent composition of each phase. These results suggest that GPI-anchored proteins such as BIAP may contribute to the recruitment of their own microdomain environment. The same team investigated the temperature-dependency of the GPI-BIAP localization in model raft supported membranes made of POPC/SM/Chol [129]. The inserted BIAP was localized in the SM/Chol enriched ordered domains at low temperature, while above 30 °C, BIAP redistributed and was present in both the fluid POPC enriched and the ordered SM/Chol domains. In 2008, Chiantia et al. [130] reported the importance of ceramides in the nanoscale lateral organization of the GPI-anchored placental alkaline phosphatase (GPI-PLAP) within SLBs of SM/DOPC/Chol/ceramide. AFM images revealed the specific association of PLAP with the ceramide-rich phases. The authors suggested that the specific association of GPI-PLAP with ceramide domains may be of crucial importance in the signal transduction regulation when ceramide is produced in the cell membrane.

Among the existing AFM literature on SLB–protein interactions, enzyme proteins with lipase activity have been frequently described for their membrane remodelling properties. For example, phospholipase A2 (PLA2) was shown to produce channels within lipid membranes preferentially at the border of defects [131,132]. The Bjornholm's team noted a latency period preceeding the PLA2 mediated hydrolysis of bilayers [133]. The combined kinetic and structural AFM study of the PLA2 catalyzed hydrolysis of DPPC supported bilayers revealed a lag-burst mechanism, and a preferential action of this enzyme in the defects of the membrane [134]. Another group proved the sensitivity of PLA2 for membrane lipid curvature with the help of the ripple phases formed in supported double bilayers [135].

The membrane activity of another enzyme, phospholipase D (PLD) was recently characterized [136]. PLD catalyzes the hydrolysis of the

phosphodiester bond between the phosphatidyl-moiety and the choline headgroup of PC which liberates phosphatidic acid (PA) and free choline. Two types of SLBs were prepared – continuous and patchy DPPC bilayers – to probe the influence of lipid packing on the PLD activity. PLD induced important morphological alterations of continuous membranes: initially, holes were formed and the bilayer surface was finally thickened in some areas by 2.5 nm. This blistering of the bilayer was attributed to the PLD-induced accumulation of the negatively charged lipid PA that would provoke localized charge repulsions between the bilayer and the underlying mica surface. By contrast, with the patchy DPPC system, the domain shapes were greatly modified by the enzyme activity and they evolved into elongated and melted morphologies.

More recently, AFM permitted to observe the in-situ hydrolysis of SM into ceramide catalyzed by sphingomyelinases (SMase) on SLBs composed of DOPC/SM/Chol mixtures [137,138]. When SMase was added to the bilayers, the ceramide production resulted in an enlargement of the initial ordered domains, yielding large clusters of domains. The authors correlated the formation of these large clusters to the coalescence of raft domains which finally form large signalling platforms in cell membranes.

Interestingly, some of the soluble proteins are able to interact transiently with biomembranes, and sometimes with a great biological significance. For this reason, the interaction of soluble proteins with SLBs was also probed by AFM to observe the possible modifications in the membrane structure and to identify preferential sites of binding. Saposins A, B and C are small soluble non-enzymatic glycoproteins that interact transiently with lysosomal membranes where they are required for the hydrolysis of sphingolipids by specific hydrolases. The observations at the nanometer scale of the interaction of saposins A, B and C with SLBs showed extensive reorganization of the membrane structure [139,140]. Saposins A and C induced very similar transformations corresponding to a reduction of membrane thickness, while saposin B produced nanoholes that ultimately filled with granular material, presumably proteins [139]. The authors suggested that the biological significance of the observed membrane modifications could reside in the ability of these small proteins to assemble key lipids into membrane microdomains in a spatial and temporal order which would finally activate the proper lysosomal enzymes. In addition the same team [141] showed that acid β-glucosidase, which is responsible for the hydrolysis of glucose from glucosylceramide, requires an activation by saposin C to gain access to the membrane embedded glycosphingolipid substrate.

Cytochrome *c* (cyt *c*) is another soluble protein interacting with SLBs. Cyt *c* is a small basic protein involved in the mitochondrial respiratory chain where it transfers electrons between two redox protein complexes integrated into the inner membrane, ubiquinol cyt *c* oxidoreductase (cytochrome *bc1*) and cyt *c* oxidase. A two step mechanism was previously proposed to explain the insertion of cyt *c* in membranes presenting negatively charged lipids: first, an electrostatic interaction between cyt *c* and anionic lipids at the membrane surface, then the exposure of cyt *c* hydrophobic groups to enter the membrane [142]. AFM experiments clearly proved the insertion of cyt *c* molecules inside negatively charged membranes [143]. More recently, time-lapse AFM of fluid/gel SLBs pointed out the ability of cyt *c* to alter zwitterionic membranes, in a way that was modulated by the lipid molecular packing [144]. A soluble protein complex, the 20S proteasome plays important roles in the degradation of intracellular proteins. It exhibits a peptidase activity which is activated by the binding to biomembranes. Furuike et al. [145] described the interaction of 20S proteasome with SLBs. Among the various lipid compositions they tested, the authors found a strong binding of proteasome 20S to SLBs containing phosphatidylinositol thus suggesting a specific interaction. Recently, the crucial role of the biologically important lipid L-α-phosphatidylinositol-4,5-bisphosphate (PIP_2) in the recruitment of ezrin protein at the membrane surface was directly observed by AFM [146]. Ezrin is a soluble protein acting as a membrane-cytoskeletal linker. Indeed, the structure of ezrin presents two domains: one domain binds specifically to the membrane lipid PIP_2 and the other domain connects with F-actin molecules from the cytoskeleton. AFM images clearly evidenced a cooperative binding of ezrin to PIP_2, which permitted to propose two different mechanisms: (i) a lateral growing of ezrin clusters on the membrane by the progressive recruitment of the proteins, and (ii) a piggy-back model corresponding to the binding of ezrin molecules ontop of the clusters. The piggy-back association of ezrin molecules would then evolve by the sliding of the proteins to obtain a monolayer of clustered ezrin on the membrane.

An exciting issue for future work is to design and investigate SLBs that incorporate proteins with large extra-membrane domains, using tethered bilayers or polymer supported bilayers. Although AFM imaging of such systems has been reported [147–150], progress in this area is clearly needed.

6. AFM tracks nanoscale bilayer–drug interactions

Currently, there is much interest in understanding drug–membrane interactions at the molecular level. In pharmacology, it is well-known that the structure and properties of biological membranes can be strongly affected by their interaction with drugs; in turns, this interaction modulates the drug activity and toxicity [151–153]. The conformation of acyl groups, the membrane surface and thickness, the phase transistion temperature, the membrane potential and hydration of head groups and the membrane fusion properties are just a few examples of traits that can be modified upon interaction with drugs. Membrane domains such as lipid rafts may have a number of important consequences on this interaction, including enhancement of penetration and insertion of the molecules at the domain boundary.

AFM offers exciting possibilities to monitor the dynamic remodelling of bilayers upon interaction with drugs [154–160]. For instance, incubation of DOPC/DPPC bilayers with the dicationic antibiotic azithromycin was found to induce progressive erosion and disappearance of DPPC gel domains within 60 min (Fig. 6) [154]. This effect was attributed to the disruption of the tight molecular packing of the DPPC molecules by the drug, in agreement with earlier biophysical experiments. By contrast, SM and SM/Chol domains mimicking lipid rafts were not modified by azithromycin. This higher membrane stability was suggested to reflect stronger intermolecular interactions between sphingomyelin molecules.

The interaction of two fluoroquinolones, ciprofloxacin and moxifloxacin, with lipids was probed using an array of complementary techniques [155]. Moxifloxacin induced, to a larger extent than ciprofloxacin, an erosion of the DPPC domains (AFM images) and a shift of the surface pressure–area isotherms of DOPC/DPPC/fluoroquinolone monolayers towards a lower area per molecule (Langmuir studies). These effects were related to a lower propensity of moxifloxaxin to be released from the lipid to the aqueous phase (phase transfer studies and conformational analysis) and a marked decrease of all-trans conformation of acyl lipid chains of DPPC (ATR-FTIR) without increase of lipid disorder and change in the tilt between the normal and the germanium surface (ATR-FTIR). All together, the different behaviour of ciprofloxacin, compared to moxifloxacin, in terms of interactions with lipids could explain differences in their cellular accumulation and therefore their activity against intracellular bacteria. Another team used SLBs made of *E. coli* lipid extracts to study the interaction with the antibiotics ciprofloxacin and two derivatives [156]. AFM and fluorescence spectroscopy experiments proved the formation of pores in the presence of ciprofloxacin. Filipin, a polyene antibiotic, was shown to promote the formation of aggregates in cholesterol containing membranes [157,158]. Incubation of Filipin with DOPC/SM bilayers containing 10% Chol produced highly ordered striated patterns having a periodicity of 4.3 nm [158].

Anesthetics constitute another important class of drugs which have attracted much interest. Here, an important question is to understand

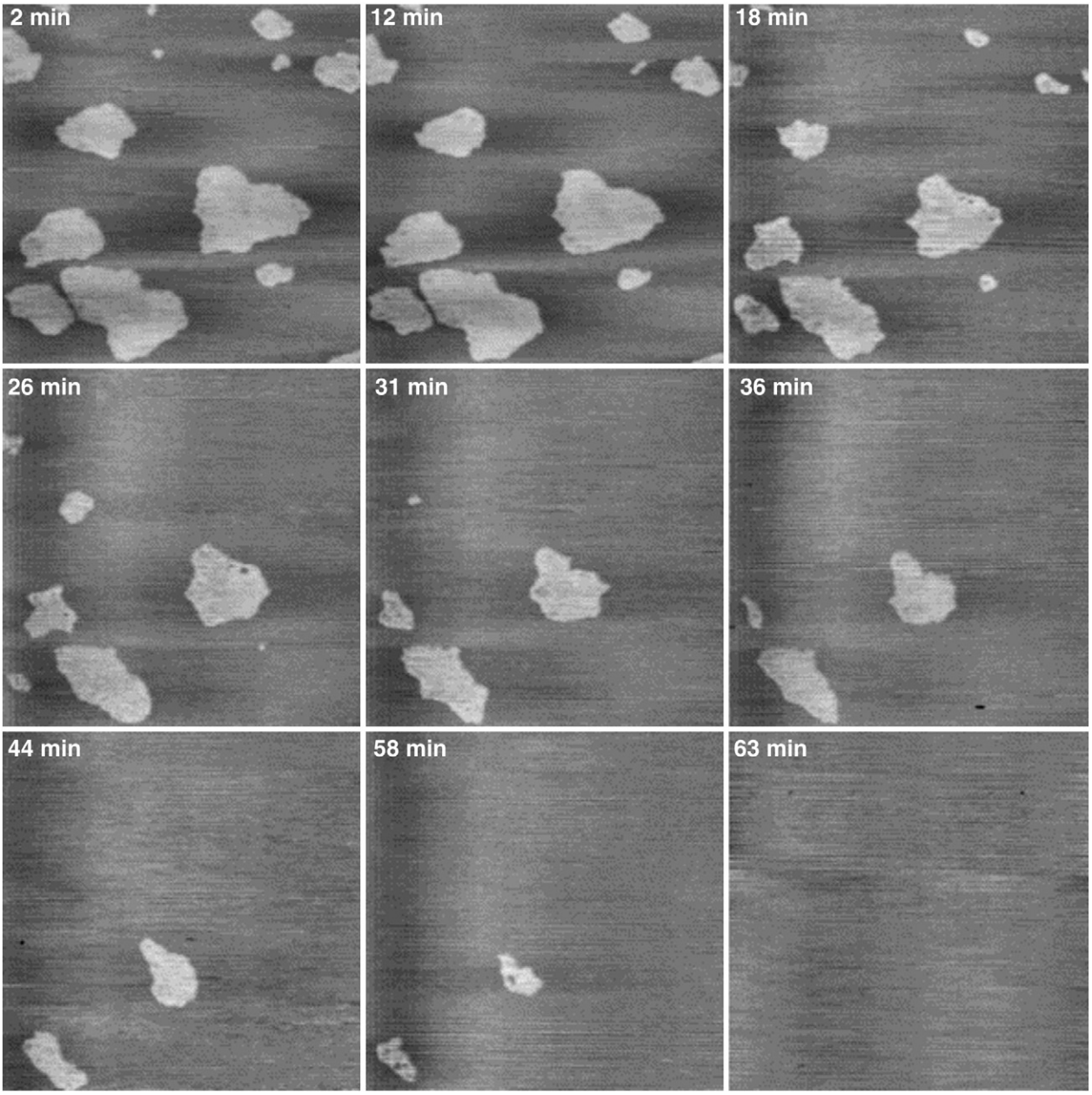

Fig. 6. Effect of azithromycin on mixed fluid/gel bilayers. AFM height images (7.5×7.5 μm; *z*-scale: 10 nm) of a mixed DPPC/DOPC (1:1, mol/mol) bilayer recorded in an azithromycin solution (1 mM) at increasing incubation times. Reprinted with permission from [154]. Copyright 2004 Elsevier Science Ltd.

their mode of action on the plasma membrane of neurons. The action of anesthetics can be explained, at least for a part, by the modification of the lipid packing, the degree of motional disorder in lipid chains, and the polarization of the membranes. The interaction of anesthetics such as halothane and dibucaine has been investigated by AFM [159,160]. Halothane was shown to promote the interdigitation in some areas of DPPC bilayers [159]. The molecular packing of Egg PC and DMPC bilayers was modified by the interaction of dibucaine with the polar head groups of the lipids [160]. By increasing incubation times and dibucain concentration, SLBs were solubilized, an effect attributed to dibucain-induced changes in the local curvature of the lipid bilayer.

7. AFM investigations of membrane–nanoparticle interactions

Owing to their remarkable properties, nanoparticles (NPs) are widely used for electrical, mechanical, magnetic, optical, therapeutic, catalytic and cosmetic applications [161]. Sometimes, however, such NPs can be released in the environment thereby raising questions about pollution and health risks. NPs particularly hold exciting promises in biomedical applications such as medical imaging and drug/gene delivery [162–164]. Their future development therefore relies on our understanding of their interactions not only with specific biological targets, but also with biomembranes.

Dendrimers are a promising class of NPs suitable for many biological applications [165–167]. For instance, dendritic polymers can be easily stimulated selectively to release drugs. The interactions of polycationic dendrimers and SLBs have been extensively studied by the Banaszak Holl's team [168–173]. They examined the effects of poly (amidoamine) (PAMAM) dendrimers on DMPC supported bilayers. PAMAM dendrimers of high generation (G7) terminated by amine or carboxyl caused the formation and growth of nanoscale holes as observed by time-lapse AFM [168]. Conversely, G5 PAMAM dendrimers and tectodendrimer clusters did not cause the formation holes [168] but they expanded the size of pre-existing defects in the bilayer.

No modification of the DMPC bilayer was observed with the amine terminated G3 PAMAM dendrimers [170,173]. When the G7 PAMAM dendrimers were modified by capping the charged groups with acetamide functions, all their effects on membrane were canceled [170]. The authors proposed that the dendrimers were able to collect lipids from the membrane surface, thereby forming holes and dendrimer-filled vesicles. The G5 and G7 PAMAM dendrimers were also studied in interaction with bilayers composed of a lipid extract from lung alveoli enriched in DPPC and 1-palmitoyl-2-oleoyl-sn-glycero-3-[phospho-*rac*-1-glycerol] (POPG) [174]. The two dendrimers removed lipids from the fluid domains at a significantly greater rate than for the gel domains. Parimi et al. [175] compared the effect of three sizes of PAMAM dendrimers on DMPC bilayers by combining AFM and optical waveguide lightmode spectroscopy (OWLS). They determined that the rate constant for bilayer removal follows the order G6>G4>G2 while the rate constant for adsorption follows the order G2>G4>G6. These findings may be of great interest for the design of dendrimers for specific pharmaceutical applications such as drug delivery vehicles, transfection agents or antimicrobials.

The effect of two inorganic NPs, Au–NH_2 and silica–NH_2, on DMPC bilayers was studied [173]. The NH_2-coated gold NPs caused the expansion of pre-existing defects and the silica–NH_2 particles formed bilayer holes, thus pointing out the importance of the NP carrying the amine groups.

Carbon NPs constitute another great class of NPs composed of carbon black, fullerenes and carbon nanotubes. The interaction of water soluble fullerenes with SLBs containing zwitterionic or cationic lipids was examined recently [176]. The fullerenes accumulated at the surface of the membranes, with no influence of the lipid charge. There was no modification of the bilayer thickness or morphology, suggesting that fullerene aggregates interacted with the polar head of the lipids exclusively. These findings on carbon NPs–biomembrane interactions are of biomedical significance since this class of NPs is increasingly used in manufactured products and could have toxicological consequences.

8. Imaging membrane-associated proteins

A crucial challenge in current biophysical research is to analyze membranes that are more biologically relevant, i.e. that incorporate membrane proteins which play essential roles in cellular processes and are highly relevant to human physiology and disease. AFM has been used to image a variety of membrane proteins organized into two-dimensional arrays such as, ion pumps such as bacteriorhodopsin [177,178], halorhodopsin [179,180], hexagonally packed intermediate (HPI) layers from *Deinococcus radiodurans* [177], channels (aquaporins [181,182], voltage-dependent anion channel (VDAC) [183]) and connexons [182,184]. Several elegant studies have focused on the photosynthetic apparatus of different photosynthetic bacteria, including *Rhodopseudomonas viridis* [185], *Rhodospirillum photometricum* [186,187], *Rhodobacter sphaeroides* [188], *Rhodobacter blasticus* [189] and *Rhodopseudomonas palustris* [190]. These AFM analyses provide new insight on the supramolecular organization of photosynthetic transmembrane protein complexes in native membranes. In one such study, Scheuring and Sturgis [187] investigated how the composition and architecture of photosynthetic membranes of *R. photometricum* change in response to light. Despite large modifications in the membrane composition, the local environment of core complexes remained unaltered, whereas specialized paracrystalline light-harvesting antenna domains grew under low-light conditions. It was concluded that such structural adaptation ensures efficient photon capture under low-light conditions and prevents photodamage under high-light conditions.

A number of proteins are able to form two-dimensional crystals after simple incubation with preformed SLBs. These include toxins (*Bacillus thuringiensis* toxin (Cry1Aa) [191], cholera toxin [192], α-hemolysin [193,194], perfringolysin O [195], pertussis toxin [196] and the vacuolating toxin from *Helicobacter pylori* [197]), streptavidin [198] and annexin A5 [199–202]. For example, Mou et al. [192] studied the interaction of the cholera toxin B-oligomer on a preformed SLB composed of PC and the monosialotetrahexosylganglioside GM1. They observed the spontaneous association of the proteins with the ganglioside in a two-dimensional array allowing a resolution in the range of 1 to 2 nm. In 2004, Czajkowsky et al. [195] reported the direct insertion of perfringolysin O (PFO), a cholesterol-dependent cytolysin able to form β-barrel pores in the membrane, into preformed SLBs. They prepared the membrane by transferring a first monolayer of pure PC and a second monolayer of mixed PC/Chol and then the PFO was added to the bilayer. PFO formed complexes of high density associated to the membrane. Two kinds of structures were distinguished: prepore and pore. The complexes were organized mainly in rings or arcs and the center-to-center distances between the neighboring ring complexes were estimated to 38 ± 2 nm and 37 ± 3 nm for prepores and pores respectively. By reducing the sole disulfide bond of PFO (Cys 57–Cys 190) with the reducing agent dithiotreitol (DTT), the authors observed the real-time mechanism of transition from prepore-to-pore which corresponds to a vertical collapse of the protein into the bilayer.

Sometimes, a detergent-mediated reconstitution within lipid vesicles is first required before the fusion step on the solid support. This is the case for some ion pumps (bacteriorhodopsin [203] and proteorhodopsin [204]), channels (potassium channel [205] and chloride channel [206]), sodium-proton antiporters (NhaA) [207], porin outer membrane protein F (OmpF) [208], water channel aquaporin Z [209] and ATP synthases [210–212]. Concerning the mitochondrial ATP synthase, Arechaga and Fotiadis [212] described two methods to reconstitute mitochondrial F_1F_o-ATP synthase into lipid bilayers suitable for structure analysis by electron microscopy and AFM. Proteoliposomes densely packed with bovine heart mitochondrial F_1F_o-ATP synthase were obtained by removal of the detergent molecules from ternary mixtures of lipid, detergent and protein. AFM images revealed the formation of two populations of bilayers: patches with unidirectionally inserted proteins and patches with bidirectionally oriented F_1F_o-ATPase. The second method described by these authors allowed to obtain two-dimensional crystals of recombinant hexahistidine-tagged yeast F_1F_o-ATP synthase by using the supported monolayer technique. Briefly, a monolayer of Ni-NTA-DOGS lipid (1,2-dioleoyl-*sn*-glycero-3-[(N-(5-amino-1-carboxypentyl)iminodiacetic acid)succinyl]) was spread at the air–water interface of a Teflon well. Then a ternary mixture of lipid, detergent and protein was injected in the subphase allowing the specific interaction of the His-tagged F_1F_o-ATP synthase with the Ni-NTA on the lipid at the air–water interface. Biobeads were added to the subphase to remove the detergent from the membrane. These conditions yielded the best and the most ordered 2D crystals: ATP synthases were oriented unidirectionally. TEM images indicated a hexagonal packing of the yeast F_1F_o-ATPase molecules, unit cell parameters of $a = b = 115$ Å, $\gamma = 60°$ containing one F_1F_o-ATP synthase molecule with a diffraction resolution of 29 Å.

Finally, an elegant alternative approach is to incorporate membrane proteins into preformed SLBs destabilized by detergents used in membrane biochemistry (DDM or DOTM). Milhiet et al. [92] achieved successful reconstitution of membrane proteins from the bacterial photosynthetic apparatus into preformed DOPC/DPPC bilayers. The authors reconstituted the light-harvesting complex 2 (LH2) and the core complex composed of the light-harvesting complex 1 (LH1) and the reaction center (RC) from *Rhodobacter sphaeroides*, and they also examined the core complex (LH1-RC) from *Rhodobacter veldkampii*. AFM height measurements revealed that all the proteins were incorporated unidirectionally in the lipid bilayer. AFM images showed the organization of the LH1 (top ring diameter of 9.2 ± 1.2 nm) structured in 16 α/β-heterodimers, and the nonameric subunits organization of LH2

(top ring diameter of 5.1 ± 0.27 nm). After one day, the samples evolved toward the formation of closely packed areas of protein complexes suitable for high-resolution AFM imaging. The same team investigated the effect of Ca^{2+} on the direct reconstitution of membrane proteins into preformed SLBs [93]. Here, various detergents of low CMC were tested to insert the protein complex LH1-RC. The results demonstrated that the nature of the detergent had no influence on the reconstitution, but the calcium decreased the insertion of low CMC detergents into SLBs, thereby inhibiting the protein insertion. A major advantage of this method is the extremely small amount (~1 pmol) of protein needed to obtain a high protein density in the lipid bilayer. Also, the versatility and simplicity of the technique should make it very useful for the conception of biosensors and nanobio devices involving membrane proteins.

9. Outlook

The studies reviewed here demonstrate that AFM is a powerful tool in biomembrane research, which is particularly well-suited for observing phase-separated domains on the micro and nanoscales, and for monitoring membrane remodelling and alteration upon interaction with solvents, peptides, proteins, detergents and antibiotics. Here, we surveyed recent progress in structural studies using AFM. However, it should be realized that AFM is more than a microscope. When used in the force spectroscopy mode [35], AFM enables researchers to probe a variety of physical properties, like adhesion, elasticity, and biomolecular interactions associated with lipid membranes [10,40,42]. In the future, we anticipate this modality will be increasingly used in SLB research.

AFM analyses are limited by the need to firmly attach specimens onto solid supports, meaning the very central notion of a free-standing biomembrane separating two aqueous compartments is not preserved. As a result, membrane properties such as elasticity, fluidity and diffusion properties may be altered, therefore limiting the biological relevance of the measurements. To solve this problem, membranes can be adsorbed on supports that have well-defined pores [213,214] or holes [125]. In doing so, Goncalves et al. [125] developed a novel two-chamber AFM set-up which allows membrane proteins separating two aqueous compartments to be investigated. This set-up was used to image the inner and outer surfaces of non-supported *Corynebacterium glutamicum* membranes at a resolution of ~15 Å, and to determine the elastic properties and energy of interaction of the membrane proteins. In the future, this device should allow to couple structural and functional AFM analyses of non-supported biomembranes, enabling us for instance to observe how ion, pH, and solute-gradients affect the conformation of channels, pumps and receptors.

Another crucial challenge in future nanoscale membrane research is to combine AFM with other advanced surface probing techniques. Burns [215] reported the first analysis of bilayer domains using combined AFM and fluorescence imaging. Lipids labeled by fluorescent probes enabled domain contrast in fluorescence imaging on the basis of partitioning between gel DPPC and fluid DOPC phases. Correlation with AFM topographic information revealed that they do not always faithfully report exact gel domain size or shape. Furthermore, the fluorescence contrast decreased significantly with domain size, such that small domains observed with AFM were not observed in fluorescence images despite adequate optical resolution. Fluorescence correlation spectroscopy (FCS) combined with AFM give access to structural information and to local dynamic properties [216]. This combination has been widely used by the Schwille's group to study the partitioning of lipids and proteins into SLBs [63,64].

Traditionally, the resolution in fluorescence microscopy is limited by the wavelength of light, and is usually around 200 nm. Recently, however, remarkable progress in breaking the diffraction barrier has pushed fluorescence microscopy to the exciting new era of optical nanoscopy [217,218]. In membrane research, the Hell's team recently demonstrated the ability of stimulated emission depletion (STED) far-field fluorescence nanoscopy to detect single diffusing (lipid) molecules in nanosized areas in the plasma membrane of living cells. Unlike phosphoglycerolipids, sphingolipids and glycosylphosphatidylinositol-anchored proteins were found to be transiently trapped in cholesterol-mediated molecular complexes dwelling within <20 nm diameter areas.

Lastly, we anticipate that another challenging task will be to combine structural analyses by AFM with quantitative studies of the chemical composition of lipid domains, using e.g. high-resolution imaging secondary ion mass spectrometry (SIMS) techniques [219]. The lateral resolution of this nano-SIMS method is only 50 nm, suggesting it should find broad applications in future membrane research. Recently, the nano-SIMS technique has been used on model membranes to study the localization of SM in cholesterol domains [220].

Acknowledgements

This work was supported by the National Foundation for Scientific Research (FNRS), the Université catholique de Louvain (Fonds Spéciaux de Recherche), the Région wallonne, the Federal Office for Scientific, Technical and Cultural Affairs (Interuniversity Poles of Attraction Programme), and the Research Department of the Communauté française de Belgique (Concerted Research Action). Y.F.D. is Senior Research Associate at the FNRS. Support from the following institutions is also gratefully acknowledged: The Université de Technologie de Compiègne, the French Ministry of Research (PPF BIOMIM) and the French Region Picardie.

References

[1] E. Sackmann, Supported membranes: scientific and practical applications, Science 271 (1996) 43–48.
[2] E.T. Castellana, P.S. Cremer, Solid supported lipid bilayers: from biophysical studies to sensor design, Surf. Sci. Rep. 61 (2006) 429–444.
[3] B. Schuster, U.B. Sleytr, Biomimetic S-layer supported lipid membranes, Curr. Nanosci. 2 (2006) 143–152.
[4] Y.H. Chan, S.G. Boxer, Model membrane systems and their applications, Curr. Opin. Chem. Biol. 11 (2007) 581–587.
[5] E. Reimhult, K. Kumar, Membrane biosensor platforms using nano- and microporous supports, Trends Biotechnol. 26 (2008) 82–89.
[6] C. Peetla, A. Stine, V.D. Labhasetwar, Biophysical interactions with model lipid membranes: applications in drug discovery and drug delivery, Mol. Pharm. 6 (5) (2009) 1264–1276.
[7] A. Ulman, Ultrathin organic films, Academic Press, San Diego, 1991.
[8] V. Vie, M. Van Mau, E. Lesniewska, J.P. Goudonnet, F. Heitz, C. Le Grimellec, Distribution of ganglioside GM1 between two component, two-phase phosphatidylcholine monolayers, Langmuir 14 (1998) 4574–4583.
[9] H.A. Rinia, R.A. Demel, J.P. van der Eerden, B. de Kruijff, Blistering of Langmuir–Blodgett bilayers containing anionic phospholipids as observed by atomic force microscopy, Biophys. J. 77 (1999) 1683–1693.
[10] Y.F. Dufrene, W.R. Barger, J.-B.D. Green, G.U. Lee, Nanometer-scale surface properties of mixed phospholipid monolayers and bilayers, Langmuir 13 (1997) 4779–4784.
[11] R.G. Horn, Direct measurement of the force between two lipid bilayers and observation of their fusion, Biochim. Biophys. Acta 778 (1984) 224–228.
[12] A.A. Brian, H.M. McConnell, Allogeneic stimulation of cytotoxic T cells by supported planar membranes, Proc. Natl. Acad. Sci. U. S. A. 81 (1984) 6159–6163.
[13] J. Jass, T. Tjarnhage, G. Puu, From liposomes to supported, planar bilayer structures on hydrophilic and hydrophobic surfaces: an atomic force microscopy study, Biophys. J. 79 (2000) 3153–3163.
[14] R.P. Richter, A.R. Brisson, Following the formation of supported lipid bilayers on mica: a study combining AFM, QCM-D, and ellipsometry, Biophys. J. 88 (2005) 3422–3433.
[15] R. Richter, A. Mukhopadhyay, A. Brisson, Pathways of lipid vesicle deposition on solid surfaces: a combined QCM-D and AFM study, Biophys. J. 85 (2003) 3035–3047.
[16] R.P. Richter, R. Berat, A.R. Brisson, Formation of solid-supported lipid bilayers: an integrated view, Langmuir 22 (2006) 3497–3505.
[17] M. Przybylo, J. Sykora, J. Humpolickova, A. Benda, A. Zan, M. Hof, Lipid diffusion in giant unilamellar vesicles is more than 2 times faster than in supported phospholipid bilayers under identical conditions, Langmuir 22 (2006) 9096–9099.
[18] U. Mennicke, T. Salditt, Preparation of solid-supported lipid bilayers by spin-coating, Langmuir 18 (2002) 8172–8177.
[19] A.C. Simonsen, L.A. Bagatolli, Structure of spin-coated lipid films and domain formation in supported membranes formed by hydration, Langmuir 20 (2004) 9720–9728.

[20] G. Pompeo, M. Girasole, A. Cricenti, F. Cattaruzza, A. Flamini, T. Prosperi, J. Generosi, A.C. Castellano, AFM characterization of solid-supported lipid multilayers prepared by spin-coating, Biochim. Biophys. Acta 1712 (2005) 29–36.
[21] S. Chiantia, N. Kahya, P. Schwille, Dehydration damage of domain-exhibiting supported bilayers: an AFM study on the protective effects of disaccharides and other stabilizing substances, Langmuir 21 (2005) 6317–6323.
[22] S.V. Bennun, R. Faller, M.L. Longo, Drying and rehydration of DLPC/DSPC symmetric and asymmetric supported lipid bilayers: a combined AFM and fluorescence microscopy study, Langmuir 24 (2008) 10371–10381.
[23] J.P. Slotte, Direct observation of the action of cholesterol oxidase in monolayers, Biochim. Biophys. Acta 1259 (1995) 180–186.
[24] D. Honig, D. Mobius, Direct visualization of monolayers at the air–water-interface by Brewster-angle microscopy, J. Phys. Chem. 95 (1991) 4590–4592.
[25] K. Kago, H. Matsuoka, R. Yoshitome, H. Yamaoka, K. Ijiro, M. Shimomura, Direct in situ observation of a lipid monolayer–DNA complex at the air–water interface by X-ray reflectometry, Langmuir 15 (1999) 5193–5196.
[26] H. Möhwald, Direct characterization of monolayers at the air–water interface, Thin Solid Films 159 (1988) 1–15.
[27] H. Reinl, T. Brumm, T.M. Bayerl, Changes of the physical properties of the liquid-ordered phase with temperature in binary mixtures of DPPC with cholesterol: a H-NMR, FT-IR, DSC, and neutron scattering study, Biophys. J. 61 (1992) 1025–1035.
[28] A. Grelard, A. Couvreux, C. Loudet, E.J. Dufourc, Solution and solid-state NMR of lipids, Methods Mol. Biol. 462 (2009) 111–133.
[29] B. Bechinger, The structure, dynamics and orientation of antimicrobial peptides in membranes by multidimensional solid-state NMR spectroscopy, Biochim. Biophys. Acta 1462 (1999) 157–183.
[30] Y.F. Dufrene, T. Boland, J.W. Schneider, W.R. Barger, G.U. Lee, Characterization of the physical properties of model biomembranes at the nanometer scale with the atomic force microscope, Faraday Discuss. 111 (1998) 79–94.
[31] M. Deleu, M. Paquot, P. Jacques, P. Thonart, Y. Adriaensen, Y.F. Dufrene, Nanometer scale organization of mixed surfactin/phosphatidylcholine monolayers, Biophys. J. 77 (1999) 2304–2310.
[32] V. Schram, H.N. Lin, T.E. Thompson, Topology of gel-phase domains and lipid mixing properties in phase-separated two-component phosphatidylcholine bilayers, Biophys. J. 71 (1996) 1811–1822.
[33] R. Linton, V. Guarisco, J.J. Lee, B. Hagenhoff, A. Benninghoven, Analytical surface spectroscopy of phospholipid Langmuir–Blodgett-films, Thin Solid Films 210 (1992) 565–570.
[34] G. Binnig, C.F. Quate, C. Gerber, Atomic force microscope, Phys. Rev. Lett. 56 (1986) 930–933.
[35] D.J. Muller, Y.F. Dufrene, Atomic force microscopy as a multifunctional molecular toolbox in nanobiotechnology, Nat. Nanotechnol. 3 (2008) 261–269.
[36] Y.F. Dufrene, Towards nanomicrobiology using atomic force microscopy, Nat. Rev. Microbiol. 6 (2008) 674–680.
[37] J. Schneider, Y.F. Dufrene, W.R. Barger Jr, G.U. Lee, Atomic force microscope image contrast mechanisms on supported lipid bilayers, Biophys. J. 79 (2000) 1107–1118.
[38] J. Schneider, W. Barger, G.U. Lee, Nanometer scale surface properties of supported lipid bilayers measured with hydrophobic and hydrophilic atomic force microscope probes, Langmuir 19 (2003) 1899–1907.
[39] S. Kunneke, D. Kruger, A. Janshoff, Scrutiny of the failure of lipid membranes as a function of headgroups, chain length, and lamellarity measured by scanning force microscopy, Biophys. J. 86 (2004) 1545–1553.
[40] S. Garcia-Manyes, G. Oncins, F. Sanz, Effect of ion-binding and chemical phospholipid structure on the nanomechanics of lipid bilayers studied by force spectroscopy, Biophys. J. 89 (2005) 1812–1826.
[41] M.H. Abdulreda, V.T. Moy, Atomic force microscope studies of the fusion of floating lipid bilayers, Biophys. J. 92 (2007) 4369–4378.
[42] L. Picas, M.T. Montero, A. Morros, M.E. Cabanas, B. Seantier, P.E. Milhiet, J. Hernandez-Borrell, Calcium-induced formation of subdomains in phosphatidylethanolamine-phosphatidylglycerol bilayers: a combined DSC, 31P NMR, and AFM study, J. Phys. Chem. B 113 (2009) 4648–4655.
[43] R.M. Sullan, J.K. Li, S. Zou, Direct correlation of structures and nanomechanical properties of multicomponent lipid bilayers, Langmuir 25 (2009) 7471–7477.
[44] A.L. Weisenhorn, F.J. Schmitt, W. Knoll, P.K. Hansma, Streptavidin binding observed with an atomic force microscope, Ultramicroscopy 42–44 (Pt B) (1992) 1125–1132.
[45] M.-C. Giocondi, V. Vie, E. Lesniewska, P.-E. Milhiet, M. Zinke-Allmang, C. Le Grimellec, Phase topology and growth of single domains in lipid bilayers, Langmuir 17 (2001) 1653–1659.
[46] M.C. Giocondi, S. Boichot, T. Plenat, C.C. Le Grimellec, Structural diversity of sphingomyelin microdomains, Ultramicroscopy 100 (2004) 135–143.
[47] W.C. Lin, C.D. Blanchette, T.V. Ratto, M.L. Longo, Lipid asymmetry in DLPC/DSPC-supported lipid bilayers: a combined AFM and fluorescence microscopy study, Biophys. J. 90 (2006) 228–237.
[48] L.J. Johnston, Nanoscale imaging of domains in supported lipid membranes, Langmuir 23 (2007) 5886–5895.
[49] T. Kaasgaard, C. Leidy, J.H. Crowe, O.G. Mouritsen, K. Jorgensen, Temperature-controlled structure and kinetics of ripple phases in one- and two-component supported lipid bilayers, Biophys. J. 85 (2003) 350–360.
[50] C. Leidy, T. Kaasgaard, J.H. Crowe, O.G. Mouritsen, K. Jorgensen, Ripples and the formation of anisotropic lipid domains: imaging two-component supported double bilayers by atomic force microscopy, Biophys. J. 83 (2002) 2625–2633.
[51] M.C. Giocondi, L. Pacheco, P.E. Milhiet, C. Le Grimellec, Temperature dependence of the topology of supported dimirystoyl–distearoyl phosphatidylcholine bilayers, Ultramicroscopy 86 (2001) 151–157.
[52] C.D. Blanchette, W.C. Lin, T.V. Ratto, M.L. Longo, Galactosylceramide domain microstructure: impact of cholesterol and nucleation/growth conditions, Biophys. J. 90 (2006) 4466–4478.
[53] C.D. Blanchette, C.A. Orme, T.V. Ratto, M.L. Longo, Quantifying growth of symmetric and asymmetric lipid bilayer domains, Langmuir 24 (2008) 1219–1224.
[54] E.I. Goksu, J.M. Vanegas, C.D. Blanchette, W.C. Lin, M.L. Longo, AFM for structure and dynamics of biomembranes, Biochim. Biophys. Acta 1788 (2009) 254–266.
[55] U. Bernchou, J.H. Ipsen, A.C. Simonsen, Growth of solid domains in model membranes: quantitative image analysis reveals a strong correlation between domain shape and spatial position, J. Phys. Chem. B 113 (2009) 7170–7177.
[56] A. Choucair, M. Chakrapani, B. Chakravarthy, J. Katsaras, L.J. Johnston, Preferential accumulation of Abeta(1–42) on gel phase domains of lipid bilayers: an AFM and fluorescence study, Biochim. Biophys. Acta 1768 (2007) 146–154.
[57] R.G. Anderson, The caveolae membrane system, Annu. Rev. Biochem. 67 (1998) 199–225.
[58] T. Harder, K. Simons, Caveolae, DIGs, and the dynamics of sphingolipid–cholesterol microdomains, Curr. Opin. Cell Biol. 9 (1997) 534–542.
[59] T.P.W. McMullen, R.N.A.H. Lewis, R.N. McElhaney, Cholesterol–phospholipid interactions, the liquid-ordered phase and lipid rafts in model and biological membranes, Curr. Opin. Colloid Interface Sci. 8 (2004) 459–468.
[60] H.A. Rinia, M.M. Snel, J.P. van der Eerden, B. de Kruijff, Visualizing detergent resistant domains in model membranes with atomic force microscopy, FEBS Lett. 501 (2001) 92–96.
[61] D.E. Saslowsky, J. Lawrence, X. Ren, D.A. Brown, R.M. Henderson, J.M. Edwardson, Placental alkaline phosphatase is efficiently targeted to rafts in supported lipid bilayers, J. Biol. Chem. 277 (2002) 26966–26970.
[62] W.C. Lin, C.D. Blanchette, M.L. Longo, Fluid-phase chain unsaturation controlling domain microstructure and phase in ternary lipid bilayers containing GalCer and cholesterol, Biophys. J. 92 (2007) 2831–2841.
[63] S. Chiantia, N. Kahya, J. Ries, P. Schwille, Effects of ceramide on liquid-ordered domains investigated by simultaneous AFM and FCS, Biophys. J. 90 (2006) 4500–4508.
[64] S. Chiantia, N. Kahya, P. Schwille, Raft domain reorganization driven by short- and long-chain ceramide: a combined AFM and FCS study, Langmuir 23 (2007) 7659–7665.
[65] K. El Kirat, S. Morandat, Cholesterol modulation of membrane resistance to Triton X-100 explored by atomic force microscopy, Biochim. Biophys. Acta 1768 (2007) 2300–2309.
[66] P.E. Milhiet, M.C. Giocondi, O. Baghdadi, F. Ronzon, B. Roux, C. Le Grimellec, Spontaneous insertion and partitioning of alkaline phosphatase into model lipid rafts, EMBO Rep. 3 (2002) 485–490.
[67] R.N. Kolesnick, F.M. Goni, A. Alonso, Compartmentalization of ceramide signaling: physical foundations and biological effects, J. Cell Physiol. 184 (2000) 285–300.
[68] C.R. Bollinger, V. Teichgraber, E. Gulbins, Ceramide-enriched membrane domains, Biochim. Biophys. Acta 1746 (2005) 284–294.
[69] Y.A. Hannun, Functions of ceramide in coordinating cellular responses to stress, Science 274 (1996) 1855–1859.
[70] D.A. Brown, J.K. Rose, Sorting of GPI-anchored proteins to glycolipid-enriched membrane subdomains during transport to the apical cell surface, Cell 68 (1992) 533–544.
[71] O. Domenech, L. Redondo, M.T. Montero, J. Hernandez-Borrell, Specific adsorption of cytochrome *C* on cardiolipin-glycerophospholipid monolayers and bilayers, Langmuir 23 (2007) 5651–5656.
[72] I. Reviakine, A. Simon, A. Brisson, Effect of Ca2+ on the morphology of mixed DPPC–DOPS supported phospholipid bilayers, Langmuir 16 (2000) 1473–1477.
[73] J. Mou, J. Yang, C. Huang, Z. Shao, Alcohol induces interdigitated domains in unilamellar phosphatidylcholine bilayers, Biochemistry 33 (1994) 9981–9985.
[74] R.L. Mcclain, J.J. Breen, The image-based observation of the L beta I-to-L-beta′ phase transition in solid-supported lipid bilayers, Langmuir 17 (2001) 5121–5124.
[75] J. Mou, J. Yang, Z. Shao, Tris(hydroxymethyl)aminomethane (C4H11NO3) induced a ripple phase in supported unilamellar phospholipid bilayers, Biochemistry 33 (1994) 4439–4443.
[76] S.J. Singer, G.L. Nicolson, The fluid mosaic model of the structure of cell membranes, Science 175 (1972) 720–731.
[77] K. Simons, G. van Meer, Lipid sorting in epithelial cells, Biochemistry 27 (1988) 6197–6202.
[78] K. Simons, E. Ikonen, Functional rafts in cell membranes, Nature 387 (1997) 569–572.
[79] T. Cinek, V. Horejsi, The nature of large noncovalent complexes containing glycosyl-phosphatidylinositol-anchored membrane glycoproteins and protein tyrosine kinases, J. Immunol. 149 (1992) 2262–2270.
[80] D.A. Brown, E. London, Structure and function of sphingolipid- and cholesterol-rich membrane rafts, J. Biol. Chem. 275 (2000) 17221–17224.
[81] K. Simons, D. Toomre, Lipid rafts and signal transduction, Nat. Rev. Mol. Cell Biol. 1 (2000) 31–39.
[82] W.I. Lencer, D. Saslowsky, Raft trafficking of AB5 subunit bacterial toxins, Biochim. Biophys. Acta 1746 (2005) 314–321.
[83] D.R. Taylor, N.M. Hooper, The prion protein and lipid rafts, Mol. Membr. Biol. 23 (2006) 89–99.
[84] R.J. Schroeder, E. London, D.A. Brown, Insaturations between saturated acyl chains confer detergent resistance on lipids and glycosylphosphatidylinositol (GPI)-anchored proteins: GPI-anchored proteins in liposomes and cells show similar behaviour, Proc. Natl. Acad. Sci. U. S. A. 91 (1994) 12130–12134.
[85] L.J. Pike, X. Han, K.N. Chung, R.W. Gross, Lipid rafts are enriched in arachidonic acid and plasmenylethanolamine and their composition is independent of

caveolin-1 expression: a quantitative electrospray ionization/mass spectrometric analysis, Biochemistry 41 (2002) 2075–2088.
[86] S. Bonnin, K. El Kirat, M. Becchi, M. Dubois, C. Grangeasse, C. Giraud, A.F. Prigent, M. Lagarde, B. Roux, F. Besson, Protein and lipid analysis of detergent-resistant membranes isolated from bovine kidney, Biochimie 85 (2003) 1237–1244.
[87] M.L. Jackson, C.F. Schmidt, D. Lichtenberg, B.J. Litman, A.D. Albert, Solubilization of phosphatidylcholine bilayers by octyl glucoside, Biochemistry 21 (1982) 4576–4582.
[88] J.L. Rigaud, M.T. Paternostre, A. Bluzat, Mechanisms of membrane protein insertion into liposomes during reconstitution procedures involving the use of detergents. 2. Incorporation of the light-driven proton pump bacteriorhodopsin, Biochemistry 27 (1988) 2677–2688.
[89] M.T. Paternostre, M. Roux, J.L. Rigaud, Mechanisms of membrane protein insertion into liposomes during reconstitution procedures involving the use of detergents. 1. Solubilization of large unilamellar liposomes (prepared by reverse-phase evaporation) by Triton X-100, octyl glucoside, and sodium cholate, Biochemistry 27 (1988) 2668–2677.
[90] S. Morandat, K. El Kirat, Membrane resistance to Triton X-100 explored by real-time atomic force microscopy, Langmuir 22 (2006) 5786–5791.
[91] S. Morandat, K. El Kirat, Solubilization of supported lipid membranes by octyl glucoside observed by time-lapse atomic force microscopy, Colloids Surf. B 55 (2007) 179–184.
[92] P.E. Milhiet, F. Gubellini, A. Berquand, P. Dosset, J.L. Rigaud, C. Le Grimellec, D. Levy, High-resolution AFM of membrane proteins directly incorporated at high density in planar lipid bilayer, Biophys. J. 91 (2006) 3268–3275.
[93] A. Berquand, D. Levy, F. Gubellini, C. Le Grimellec, P.E. Milhiet, Influence of calcium on direct incorporation of membrane proteins into in-plane lipid bilayer, Ultramicroscopy 107 (2007) 928–933.
[94] K. El Kirat, A. Pardo-Jacques, S. Morandat, Interaction of non-ionic detergents with biomembranes at the nanoscale observed by atomic force microscopy, Int. J. Nanotechnol. 5 (2008) 769–783.
[95] H.A. Rinia, R.A. Kik, R.A. Demel, M.M. Snel, J.A. Killian, J.P. van Der Eerden, B. de Kruijff, Visualization of highly ordered striated domains induced by transmembrane peptides in supported phosphatidylcholine bilayers, Biochemistry 39 (2000) 5852–5858.
[96] H.A. Rinia, J.W. Boots, D.T. Rijkers, R.A. Kik, M.M. Snel, R.A. Demel, J.A. Killian, J.P. van der Eerden, B. de Kruijff, Domain formation in phosphatidylcholine bilayers containing transmembrane peptides: specific effects of flanking residues, Biochemistry 41 (2002) 2814–2824.
[97] L. Lins, M. Decaffmeyer, A. Thomas, R. Brasseur, Relationships between the orientation and the structural properties of peptides and their membrane interactions, Biochim. Biophys. Acta 1778 (2008) 1537–1544.
[98] R.M. Epand, H.J. Vogel, Diversity of antimicrobial peptides and their mechanisms of action, Biochim. Biophys. Acta 1462 (1999) 11–28.
[99] T.B. Pedersen, T. Kaasgaard, M.O. Jensen, S. Frokjaer, O.G. Mouritsen, K. Jorgensen, Phase behavior and nanoscale structure of phospholipid membranes incorporated with acylated C14-peptides, Biophys. J. 89 (2005) 2494–2503.
[100] J. Mou, D.M. Czajkowsky, Z. Shao, Gramicidin A aggregation in supported gel state phosphatidylcholine bilayers, Biochemistry 35 (1996) 3222–3226.
[101] C. Steinem, H.J. Galla, A. Janshoff, Interaction of melittin with solid supported membranes, Phys. Chem. Chem. Phys. 2 (2000) 4580–4585.
[102] A. Mecke, D.K. Lee, A. Ramamoorthy, B.G. Orr, M.M. Banaszak Holl, Membrane thinning due to antimicrobial peptide binding: an atomic force microscopy study of MSI-78 in lipid bilayers, Biophys. J. 89 (2005) 4043–4050.
[103] J.E. Shaw, J.R. Alattia, J.E. Verity, G.G. Prive, C.M. Yip, Mechanisms of antimicrobial peptide action: studies of indolicidin assembly at model membrane interfaces by in situ atomic force microscopy, J. Struct. Biol. 154 (2006) 42–58.
[104] R.F. Epand, C.M. Yip, L.V. Chernomordik, D.L. LeDuc, Y.K. Shin, R.M. Epand, Self-assembly of influenza hemagglutinin: studies of ectodomain aggregation by in situ atomic force microscopy, Biochim. Biophys. Acta 1513 (2001) 167–175.
[105] R. Brasseur, Tilted peptides: a motif for membrane destabilization (hypothesis), Mol. Membr. Biol. 17 (2000) 31–40.
[106] R. Brasseur, T. Pillot, L. Lins, J. Vandekerckhove, M. Rosseneu, Peptides in membranes: tipping the balance of membrane stability, Trends Biochem. Sci. 22 (1997) 167–171.
[107] L. Lins, C. Flore, L. Chapelle, P.J. Talmud, A. Thomas, R. Brasseur, Lipid-interacting properties of the N-terminal domain of human apolipoprotein C-III, Protein Eng. 15 (2002) 513–520.
[108] K. El Kirat, L. Lins, R. Brasseur, Y.F. Dufrene, Fusogenic tilted peptides induce nanoscale holes in supported phosphatidylcholine bilayers, Langmuir 21 (2005) 3116–3121.
[109] N. Lev, Y. Shai, Fatty acids can substitute the HIV fusion peptide in lipid merging and fusion: an analogy between viral and palmitoylated eukaryotic fusion proteins, J. Mol. Biol. 374 (2007) 220–230.
[110] L. Chernomordik, Non-bilayer lipids and biological fusion intermediates, Chem. Phys. Lipids 81 (1996) 203–213.
[111] M.E. Haque, B.R. Lentz, Roles of curvature and hydrophobic interstice energy in fusion: studies of lipid perturbant effects, Biochemistry 43 (2004) 3507–3517.
[112] K. El Kirat, Y.F. Dufrene, L. Lins, R. Brasseur, The SIV tilted peptide induces cylindrical reverse micelles in supported lipid bilayers, Biochemistry 45 (2006) 9336–9341.
[113] M.E. Herbig, F. Assi, M. Textor, H.P. Merkle, The cell penetrating peptides pVEC and W2-pVEC induce transformation of gel phase domains in phospholipid bilayers without affecting their integrity, Biochemistry 45 (2006) 3598–3609.
[114] T. Plenat, S. Boichot, P. Dosset, P.E. Milhiet, C. Le Grimellec, Coexistence of a two-states organization for a cell-penetrating peptide in lipid bilayer, Biophys. J. 89 (2005) 4300–4309.
[115] J.D. Sipe, A.S. Cohen, Review: history of the amyloid fibril, J. Struct. Biol. 130 (2000) 88–98.
[116] C.M. Yip, J. McLaurin, Amyloid-beta peptide assembly: a critical step in fibrillogenesis and membrane disruption, Biophys. J. 80 (2001) 1359–1371.
[117] C.M. Yip, A.A. Darabie, J. McLaurin, Abeta42-peptide assembly on lipid bilayers, J. Mol. Biol. 318 (2002) 97–107.
[118] L. Zhang, J. Zhong, L. Huang, L. Wang, Y. Hong, Y. Sha, Parallel-oriented fibrogenesis of a beta-sheet forming peptide on supported lipid bilayers, J. Phys. Chem. B 112 (2008) 8950–8954.
[119] J. Zhong, W. Zheng, L. Huang, Y. Hong, L. Wang, Y. Qiu, Y. Sha, PrP106–126 amide causes the semi-penetrated poration in the supported lipid bilayers, Biochim. Biophys. Acta 1768 (2007) 1420–1429.
[120] A. Kakinuma, A. Ouchida, T. Shima, H. Sugino, M. Isono, G. Tamura, K. Arima, Confirmation of structure of surfactin by mass spectrometry, Agric. Biol. Chem. 33 (1969) 1669–1671.
[121] R. Brasseur, N. Braun, K. El Kirat, M. Deleu, M.P. Mingeot-Leclercq, Y.F. Dufrene, The biologically important surfactin lipopeptide induces nanoripples in supported lipid bilayers, Langmuir 23 (2007) 9769–9772.
[122] G. Francius, S. Dufour, M. Deleu, M. Paquot, M.P. Mingeot-Leclercq, Y.F. Dufrene, Nanoscale membrane activity of surfactins: influence of geometry, charge and hydrophobicity, Biochim. Biophys. Acta 1778 (2008) 2058–2068.
[123] M. Chen, M. Li, C.L. Brosseau, J. Lipkowski, AFM studies of the effect of temperature and electric field on the structure of a DMPC-cholesterol bilayer supported on a Au(111) electrode surface, Langmuir 25 (2009) 1028–1037.
[124] A.P. Quist, A. Chand, S. Ramachandran, C. Daraio, S. Jin, R. Lal, Atomic force microscopy imaging and electrical recording of lipid bilayers supported over microfabricated silicon chip nanopores: lab-on-a-chip system for lipid membranes and ion channels, Langmuir 23 (2007) 1375–1380.
[125] R.P. Goncalves, G. Agnus, P. Sens, C. Houssin, B. Bartenlian, S. Scheuring, Two-chamber AFM: probing membrane proteins separating two aqueous compartments, Nat. Methods 3 (2006) 1007–1012.
[126] Y.F. Dufrene, Atomic force microscopy of membrane proteins separating two aqueous compartments, Nat. Methods 3 (2006) 973–975.
[127] D. Marsh, Protein modulation of lipids, and vice-versa, in membranes, Biochim. Biophys. Acta 1778 (2008) 1545–1575.
[128] M.C. Giocondi, F. Besson, P. Dosset, P.E. Milhiet, C. Le Grimellec, Remodeling of ordered membrane domains by GPI-anchored intestinal alkaline phosphatase, Langmuir 23 (2007) 9358–9364.
[129] M.C. Giocondi, F. Besson, P. Dosset, P.E. Milhiet, C. Le Grimellec, Temperature-dependent localization of GPI-anchored intestinal alkaline phosphatase in model rafts, J. Mol. Recognit. 20 (2007) 531–537.
[130] S. Chiantia, J. Ries, G. Chwastek, D. Carrer, Z. Li, R. Bittman, P. Schwille, Role of ceramide in membrane protein organization investigated by combined AFM and FCS, Biochim. Biophys. Acta 1778 (2008) 1356–1364.
[131] M. Grandbois, H. Clausen-Schaumann, H. Gaub, Atomic force microscope imaging of phospholipid bilayer degradation by phospholipase A2, Biophys. J. 74 (1998) 2398–2404.
[132] H. Clausen-Schaumann, M. Grandbois, H.E. Gaub, Enzyme-assisted nanoscale lithography in lipid membranes, Adv. Mater. 10 (1998) 949–952.
[133] L.K. Nielsen, J. Risbo, T.H. Callisen, T. Bjornholm, Lag-burst kinetics in phospholipase A(2) hydrolysis of DPPC bilayers visualized by atomic force microscopy, Biochim. Biophys. Acta 1420 (1999) 266–271.
[134] L.K. Nielsen, K. Balashev, T.H. Callisen, T. Bjornholm, Influence of product phase separation on phospholipase A(2) hydrolysis of supported phospholipid bilayers studied by force microscopy, Biophys. J. 83 (2002) 2617–2624.
[135] C. Leidy, O.G. Mouritsen, K. Jorgensen, G.H. Peters, Evolution of a rippled membrane during phospholipase A2 hydrolysis studied by time-resolved AFM, Biophys. J. 87 (2004) 408–418.
[136] K. El Kirat, V. Dupres, Y.F. Dufrene, Blistering of supported lipid membranes induced by Phospholipase D, as observed by real-time atomic force microscopy, Biochim. Biophys. Acta 1778 (2008) 276–282.
[137] R. Ira, L.J. Johnston, Sphingomyelinase generation of ceramide promotes clustering of nanoscale domains in supported bilayer membranes, Biochim. Biophys. Acta 1778 (2008) 185–197.
[138] Ira, S. Zhou, D.M. Ramirez, S. Vanderlip, W. Ogilvie, Z.J. Jakubek, L.J. Johnston, Enzymatic generation of ceramide induces membrane restructuring: correlated AFM and fluorescence imaging of supported bilayers, J. Struct. Biol. 168 (1) (2009) 78–89.
[139] J.R. Alattia, J.E. Shaw, C.M. Yip, G.G. Prive, Direct visualization of saposin remodelling of lipid bilayers, J. Mol. Biol. 362 (2006) 943–953.
[140] H.X. You, X. Qi, L. Yu, Direct AFM observation of saposin C-induced membrane domains in lipid bilayers: from simple to complex lipid mixtures, Chem. Phys. Lipids 132 (2004) 15–22.
[141] J.R. Alattia, J.E. Shaw, C.M. Yip, G.G. Prive, Molecular imaging of membrane interfaces reveals mode of beta-glucosidase activation by saposin C, Proc. Natl. Acad. Sci. U. S. A. 104 (2007) 17394–17399.
[142] J.D. Cortese, A.L. Voglino, C.R. Hackenbrock, Multiple conformations of physiological membrane-bound cytochrome *c*, Biochemistry 37 (1998) 6402–6409.
[143] E.J. Choi, E.K. Dimitriadis, Cytochrome *c* adsorption to supported, anionic lipid bilayers studied via atomic force microscopy, Biophys. J. 87 (2004) 3234–3241.
[144] S. Morandat, K. El Kirat, Real-time atomic force microscopy reveals cytochrome *c*-induced alterations in neutral lipid bilayers, Langmuir 23 (2007) 10929–10932.
[145] S. Furuike, J. Hirokawa, S. Yamada, M. Yamazaki, Atomic force microscopy studies of interaction of the 20S proteasome with supported lipid bilayers, Biochim. Biophys. Acta 1615 (2003) 1–6.

[146] A. Herrig, M. Janke, J. Austermann, V. Gerke, A. Janshoff, C. Steinem, Cooperative adsorption of ezrin on PIP2-containing membranes, Biochemistry 45 (2006) 13025–13034.
[147] A. Zebrowska, P. Krysinski, Incorporation of Na(+), K(+)-ATP-ase into the thiolipid biomimetic assemblies via the fusion of proteoliposomes, Langmuir 20 (2004) 11127–11133.
[148] L.J. Jeuken, S.D. Connell, P.J. Henderson, R.B. Gennis, S.D. Evans, R.J. Bushby, Redox enzymes in tethered membranes, J. Am. Chem. Soc. 128 (2006) 1711–1716.
[149] A. Deniaud, C. Rossi, A. Berquand, J. Homand, S. Campagna, W. Knoll, C. Brenner, J. Chopineau, Voltage-dependent anion channel transports calcium ions through biomimetic membranes, Langmuir 23 (2007) 3898–3905.
[150] M.G. Friedrich, V.U. Kirste, J. Zhu, R.B. Gennis, W. Knoll, R.L. Naumann, Activity of membrane proteins immobilized on surfaces as a function of packing density, J. Phys. Chem. B 112 (2008) 3193–3201.
[151] J.K. Seydel, M. Wiese, Drug–membrane interactions, Wiley-VCH, Weinheim, 2002.
[152] J.K. Seydel, E.A. Coats, H.P. Cordes, M. Wiese, Drug membrane interaction and the importance for drug transport, distribution, accumulation, efficacy and resistance, Arch. Pharm. 327 (1994) 601–610.
[153] O.G. Mouritsen, K. Jorgensen, A new look at lipid–membrane structure in relation to drug research, Pharm. Res. 15 (1998) 1507–1519.
[154] A. Berquand, M.P. Mingeot-Leclercq, Y.F. Dufrene, Real-time imaging of drug–membrane interactions by atomic force microscopy, Biochim. Biophys. Acta 1664 (2004) 198–205.
[155] H. Bensikaddour, N. Fa, I. Burton, M. Deleu, L. Lins, A. Schanck, R. Brasseur, Y.F. Dufrene, E. Goormaghtigh, M.P. Mingeot-Leclercq, Characterization of the interactions between fluoroquinolone antibiotics and lipids: a multitechnique approach, Biophys. J. 94 (2008) 3035–3046.
[156] M.T. Montero, M. Pijoan, S. Merino-Montero, T. Vinuesa, J. Hernandez-Borrell, Interfacial membrane effects of fluoroquinolones as revealed by a combination of fluorescence binding experiments and atomic force microscopy observations, Langmuir 22 (2006) 7574–7578.
[157] N.C. Santos, E. Ter-Ovanesyan, J.A. Zasadzinski, M. Prieto, M.A. Castanho, Filipin-induced lesions in planar phospholipid bilayers imaged by atomic force microscopy, Biophys. J. 75 (1998) 1869–1873.
[158] J.C. Lawrence, D.E. Saslowsky, J.M. Edwardson, R.M. Henderson, Real-time analysis of the effects of cholesterol on lipid raft behavior using atomic force microscopy, Biophys. J. 84 (2003) 1827–1832.
[159] Z. Leonenko, E. Finot, D. Cramb, AFM study of interaction forces in supported planar DPPC bilayers in the presence of general anesthetic halothane, Biochim. Biophys. Acta 1758 (2006) 487–492.
[160] G.S. Lorite, T.M. Nobre, M.E. Zaniquelli, E. de Paula, M.A. Cotta, Dibucaine effects on structural and elastic properties of lipid bilayers, Biophys. Chem. 139 (2009) 75–83.
[161] R.M. Brechignac, J.K. Houdy, S. Lahmani, Nanomaterials and Nanochemistry, Springer-Verlag Berlin and Heidelberg GmbH & Co. K (2008).
[162] K. Riehemann, S.W. Schneider, T.A. Luger, B. Godin, M. Ferrari, H. Fuchs, Nanomedicine—challenge and perspectives, Angew. Chem. Int. Ed. Eng.l 48 (2009) 872–897.
[163] S.R. Popielarski, S. Hu-Lieskovan, S.W. French, T.J. Triche, M.E. Davis, A nanoparticle-based model delivery system to guide the rational design of gene delivery to the liver. 2. In vitro and in vivo uptake results, Bioconjug. Chem. 16 (2005) 1071–1080.
[164] A.U. Bielinska, A. Yen, H.L. Wu, K.M. Zahos, R. Sun, N.D. Weiner, J.R. Baker Jr, B.J. Roessler, Application of membrane-based dendrimer/DNA complexes for solid phase transfection in vitro and in vivo, Biomaterials 21 (2000) 877–887.
[165] U. Boas, P.M. Heegaard, Dendrimers in drug research, Chem. Soc. Rev. 33 (2004) 43–63.
[166] E.R. Gillies, J.M. Frechet, Dendrimers and dendritic polymers in drug delivery, Drug Discov. Today 10 (2005) 35–43.
[167] M. Manunta, P.H. Tan, P. Sagoo, K. Kashefi, A.J. George, Gene delivery by dendrimers operates via a cholesterol dependent pathway, Nucleic Acids Res. 32 (2004) 2730–2739.
[168] A. Mecke, S. Uppuluri, T.M. Sassanella, D.K. Lee, A. Ramamoorthy, J.R. Baker Jr, B.G. Orr, M.M. Banaszak Holl, Direct observation of lipid bilayer disruption by poly (amidoamine) dendrimers, Chem. Phys. Lipids 132 (2004) 3–14.
[169] S. Hong, A.U. Bielinska, A. Mecke, B. Keszler, J.L. Beals, X. Shi, L. Balogh, B.G. Orr, J.R. Baker Jr, M.M. Banaszak Holl, Interaction of poly(amidoamine) dendrimers with supported lipid bilayers and cells: hole formation and the relation to transport, Bioconjug. Chem. 15 (2004) 774–782.
[170] A. Mecke, I.J. Majoros, A.K. Patri, J.R. Baker Jr, M.M. Holl, B.G. Orr, Lipid bilayer disruption by polycationic polymers: the roles of size and chemical functional group, Langmuir 21 (2005) 10348–10354.
[171] S. Hong, J.A. Hessler, M.M. Banaszak Holl, P. Leroueil, A. Mecke, B.G. Orr, Physical interactions of nanoparticles with biological membranes: the observation of nanoscale hole formation, J. Chem. Health Safety 13 (2006) 16–20.
[172] P.R. Leroueil, S. Hong, A. Mecke, J.R. Baker Jr, B.G. Orr, M.M. Banaszak Holl, Nanoparticle interaction with biological membranes: does nanotechnology present a Janus face? Acc. Chem. Res. 40 (2007) 335–342.
[173] P.R. Leroueil, S.A. Berry, K. Duthie, G. Han, V.M. Rotello, D.Q. McNerny, J.R. Baker Jr, B.G. Orr, M.M. Holl, Wide varieties of cationic nanoparticles induce defects in supported lipid bilayers, Nano Lett. 8 (2008) 420–424.
[174] B. Erickson, S.C. DiMaggio, D.G. Mullen, C.V. Kelly, P.R. Leroueil, S.A. Berry, J.R. Baker Jr, B.G. Orr, M.M. Banaszak Holl, Interactions of poly(amidoamine) dendrimers with Survanta lung surfactant: the importance of lipid domains, Langmuir 24 (2008) 11003–11008.
[175] S. Parimi, T.J. Barnes, C.A. Prestidge, PAMAM dendrimer interactions with supported lipid bilayers: a kinetic and mechanistic investigation, Langmuir 24 (2008) 13532–13539.
[176] T.A. Spurlin, A.A. Gewirth, Effect of C60 on solid supported lipid bilayers, Nano Lett. 7 (2007) 531–535.
[177] C. Moller, M. Allen, V. Elings, A. Engel, D.J. Muller, Tapping-mode atomic force microscopy produces faithful high-resolution images of protein surfaces, Biophys. J. 77 (1999) 1150–1158.
[178] D.J. Muller, H.J. Sass, S.A. Muller, G. Buldt, A. Engel, Surface structures of native bacteriorhodopsin depend on the molecular packing arrangement in the membrane, J. Mol. Biol. 285 (1999) 1903–1909.
[179] N. Persike, M. Pfeiffer, R. Guckenberger, M. Radmacher, M. Fritz, Direct observation of different surface structures on high-resolution images of native halorhodopsin, J. Mol. Biol. 310 (2001) 773–780.
[180] D.A. Cisneros, D. Oesterhelt, D.J. Muller, Probing origins of molecular interactions stabilizing the membrane proteins halorhodopsin and bacteriorhodopsin, Structure 13 (2005) 235–242.
[181] N. Buzhynskyy, J.F. Girmens, W. Faigle, S. Scheuring, Human cataract lens membrane at subnanometer resolution, J. Mol. Biol. 374 (2007) 162–169.
[182] S. Scheuring, N. Buzhynskyy, S. Jaroslawski, R.P. Goncalves, R.K. Hite, T. Walz, Structural models of the supramolecular organization of AQP0 and connexons in junctional microdomains, J. Struct. Biol. 160 (2007) 385–394.
[183] R.P. Goncalves, N. Buzhynskyy, V. Prima, J.N. Sturgis, S. Scheuring, Supramolecular assembly of VDAC in native mitochondrial outer membranes, J. Mol. Biol. 369 (2007) 413–418.
[184] S.A. John, D. Saner, J.D. Pitts, A. Holzenburg, M.E. Finbow, R. Lal, Atomic force microscopy of arthropod gap junctions, J. Struct. Biol. 120 (1997) 22–31.
[185] S. Scheuring, J. Seguin, S. Marco, D. Levy, B. Robert, J.L. Rigaud, Nanodissection and high-resolution imaging of the *Rhodopseudomonas viridis* photosynthetic core complex in native membranes by AFM, Proc. Natl. Acad. Sci. U. S. A. 100 (2003) 1690–1693.
[186] S. Scheuring, J.L. Rigaud, J.N. Sturgis, Variable LH2 stoichiometry and core clustering in native membranes of *Rhodospirillum photometricum*, EMBO J. 23 (2004) 4127–4133.
[187] S. Scheuring, J.N. Sturgis, Chromatic adaptation of photosynthetic membranes, Science 309 (2005) 484–487.
[188] S. Bahatyrova, R.N. Frese, C.A. Siebert, J.D. Olsen, K.O. Van Der Werf, R. Van Grondelle, R.A. Niederman, P.A. Bullough, C. Otto, C.N. Hunter, The native architecture of a photosynthetic membrane, Nature 430 (2004) 1058–1062.
[189] S. Scheuring, J. Busselez, D. Levy, Structure of the dimeric PufX-containing core complex of *Rhodobacter blasticus* by in situ atomic force microscopy, J. Biol. Chem. 280 (2005) 1426–1431.
[190] S. Scheuring, R.P. Goncalves, V. Prima, J.N. Sturgis, The photosynthetic apparatus of *Rhodopseudomonas palustris*: structures and organization, J. Mol. Biol. 358 (2006) 83–96.
[191] V. Vie, N. Van Mau, P. Pomarede, C. Dance, J.L. Schwartz, R. Laprade, R. Frutos, C. Rang, L. Masson, F. Heitz, C. Le Grimellec, Lipid-induced pore formation of the *Bacillus thuringiensis* Cry1Aa insecticidal toxin, J. Membr. Biol. 180 (2001) 195–203.
[192] J. Mou, J. Yang, Z. Shao, Atomic force microscopy of cholera toxin B-oligomers bound to bilayers of biologically relevant lipids, J. Mol. Biol. 248 (1995) 507–512.
[193] Y. Fang, S. Cheley, H. Bayley, J. Yang, The heptameric prepore of a staphylococcal alpha-hemolysin mutant in lipid bilayers imaged by atomic force microscopy, Biochemistry 36 (1997) 9518–9522.
[194] M.S. Malghani, Y. Fang, S. Cheley, H. Bayley, J. Yang, Heptameric structures of two alpha-hemolysin mutants imaged with in situ atomic force microscopy, Microsc. Res. Tech. 44 (1999) 353–356.
[195] D.M. Czajkowsky, E.M. Hotze, Z. Shao, R.K. Tweten, Vertical collapse of a cytolysin prepore moves its transmembrane beta-hairpins to the membrane, EMBO J. 23 (2004) 3206–3215.
[196] J. Yang, J. Mou, Z. Shao, Structure and stability of pertussis toxin studied by in situ atomic force microscopy, FEBS Lett. 338 (1994) 89–92.
[197] D.M. Czajkowsky, H. Iwamoto, T.L. Cover, Z. Shao, The vacuolating toxin from *Helicobacter pylori* forms hexameric pores in lipid bilayers at low pH, Proc. Natl. Acad. Sci. U. S. A. 96 (1999) 2001–2006.
[198] I. Reviakine, A. Brisson, Streptavidin 2D crystals on supported phospholipid bilayers: toward constructing anchored phospholipid bilayers, Langmuir 17 (2001) 8293–8299.
[199] I. Reviakine, W. Bergsma-Schutter, A. Brisson, Growth of protein 2-D crystals on supported planar lipid bilayers imaged in situ by AFM, J. Struct. Biol. 121 (1998) 356–361.
[200] I. Reviakine, W. Bergsma-Schutter, C. Mazeres-Dubut, N. Govorukhina, A. Brisson, Surface topography of the p3 and p6 annexin V crystal forms determined by atomic force microscopy, J. Struct. Biol. 131 (2000) 234–239.
[201] I. Reviakine, W. Bergsma-Schutter, A.N. Morozov, A. Brisson, Two-dimensional crystallization of annexin A5 on phospholipid bilayers and monolayers: a solid–solid phase transition between crystal forms, Langmuir 17 (2001) 1680–1686.
[202] R.P. Richter, J.L. Him, B. Tessier, C. Tessier, A.R. Brisson, On the kinetics of adsorption and two-dimensional self-assembly of annexin A5 on supported lipid bilayers, Biophys. J. 89 (2005) 3372–3385.
[203] D.T. Kim, H.W. Blanch, C.J. Radke, Imaging of reconstituted purple membranes by atomic force microscopy, Colloids Surf. B 41 (2005) 263–276.
[204] A.L. Klyszejko, S. Shastri, S.A. Mari, H. Grubmuller, D.J. Muller, C. Glaubitz, Folding and assembly of proteorhodopsin, J. Mol. Biol. 376 (2008) 35–41.
[205] S. Jaroslawski, B. Zadek, F. Ashcroft, C. Venien-Bryan, S. Scheuring, Direct visualization of KirBac3.1 potassium channel gating by atomic force microscopy, J. Mol. Biol. 374 (2007) 500–505.

[206] H. Iwamoto, D.M. Czajkowsky, T.L. Cover, G. Szabo, Z. Shao, VacA from *Helicobacter pylori*: a hexameric chloride channel, FEBS Lett. 450 (1999) 101–104.
[207] A. Kedrov, C. Ziegler, H. Janovjak, W. Kuhlbrandt, D.J. Muller, Controlled unfolding and refolding of a single sodium-proton antiporter using atomic force microscopy, J. Mol. Biol. 340 (2004) 1143–1152.
[208] D.J. Muller, A. Engel, Voltage and pH-induced channel closure of porin OmpF visualized by atomic force microscopy, J. Mol. Biol. 285 (1999) 1347–1351.
[209] S. Scheuring, P. Ringler, M. Borgnia, H. Stahlberg, D.J. Muller, P. Agre, A. Engel, High resolution AFM topographs of the *Escherichia coli* water channel aquaporin Z, EMBO J. 18 (1999) 4981–4987.
[210] D.J. Muller, N.A. Dencher, T. Meier, P. Dimroth, K. Suda, H. Stahlberg, A. Engel, H. Seelert, U. Matthey, ATP synthase: constrained stoichiometry of the transmembrane rotor, FEBS Lett. 504 (2001) 219–222.
[211] H. Seelert, N.A. Dencher, D.J. Muller, Fourteen protomers compose the oligomer III of the proton-rotor in spinach chloroplast ATP synthase, J. Mol. Biol. 333 (2003) 337–344.
[212] I. Arechaga, D. Fotiadis, Reconstitution of mitochondrial ATP synthase into lipid bilayers for structural analysis, J. Struct. Biol. 160 (2007) 287–294.
[213] C. Hennesthal, C. Steinem, Pore-spanning lipid bilayers visualized by scanning force microscopy, J. Am. Chem. Soc. 122 (2000) 8085–8086.
[214] C. Hennesthal, J. Drexler, C. Steinem, Membrane-suspended nanocompartments based on ordered pores in alumina, Chemphyschem 3 (2002) 885–889.
[215] A.R. Burns, Domain structure in model membrane bilayers investigated by simultaneous atomic force microscopy and fluorescence imaging, Langmuir 19 (2003) 8358–8363.
[216] A.R. Burns, D.J. Frankel, T. Buranda, Local mobility in lipid domains of supported bilayers characterized by atomic force microscopy and fluorescence correlation spectroscopy, Biophys. J. 89 (2005) 1081–1093.
[217] S.W. Hell, Far-field optical nanoscopy, Science 316 (2007) 1153–1158.
[218] S.W. Hell, Microscopy and its focal switch, Nat. Methods 6 (2009) 24–32.
[219] M.L. Kraft, P.K. Weber, M.L. Longo, I.D. Hutcheon, S.G. Boxer, Phase separation of lipid membranes analyzed with high-resolution secondary ion mass spectrometry, Science 313 (2006) 1948–1951.
[220] C.M. McQuaw, L. Zheng, A.G. Ewing, N. Winograd, Localization of sphingomyelin in cholesterol domains by imaging mass spectrometry, Langmuir 23 (2007) 5645–5650.